Constraints on the carbon cycle from the NASA Carbon Monitoring System

Kevin W. Bowman
Jet Propulsion Laboratory
California Institute of Technology

CMS team:

Kevin Bowman, Junjie Liu, Nicholas Parazoo, Meemong Lee, Dimitris Menemenlis, Holger Brix, Joshua Fisher, Christian Frankenberg

Jet Propulsion Laboratory, California Institute of Technology

Joint Institute for Regional Earth System Science and Technology, University of California, Los Angeles

Steven Pawson, Lesley Ott, James Collatz, Watson Gregg, Zhengxin Zhu, Randy Kawa, Cecile Rousseaux

NASA Goddard Space Flight Center

Chris Hill, Mick Follows, Stephanie Dutkiewicz

MIT

Scott Denning, Kathy Haynes, Ian Baker

Colorado State University

Kevin Gurney

Arizona State University

Gregg Marland, Eric Marland, Chris Badurek

Appalachian State University

Daven Henze and Nicholas Bousserez

University of Colorado, Boulder

Milestone in Climate Forcing

Continuing reliance on coal, which fuels this power plant in Germany, is driving carbon dioxide levels in the atmosphere ever higher.

CLIMATE

Global carbon dioxide levels near worrisome milestone

Concentrations of greenhouse gas will soon surpass 400 parts per million at sentinel spot.

We are entering into the world of "dangerous climate change"

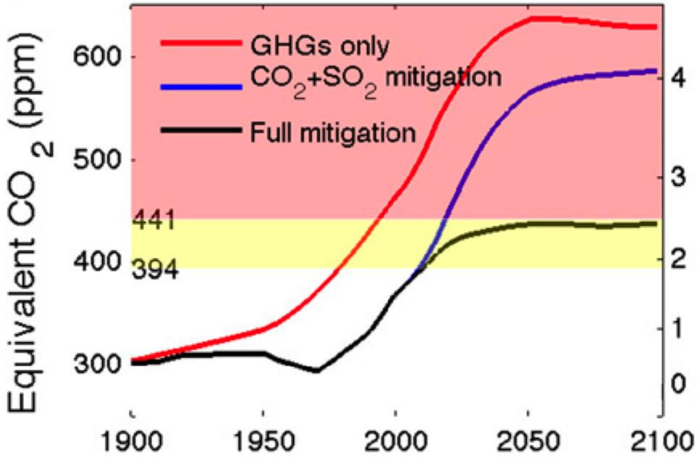

Ramanathan and Xu, PNAS (2010)

ON THE RISE

Measurements of atmospheric CO_2 levels at Mauna Loa, Hawaii, show that the greenhouse gas has accumulated steadily, and spiked above 400 parts per million (p.p.m) several times in April.

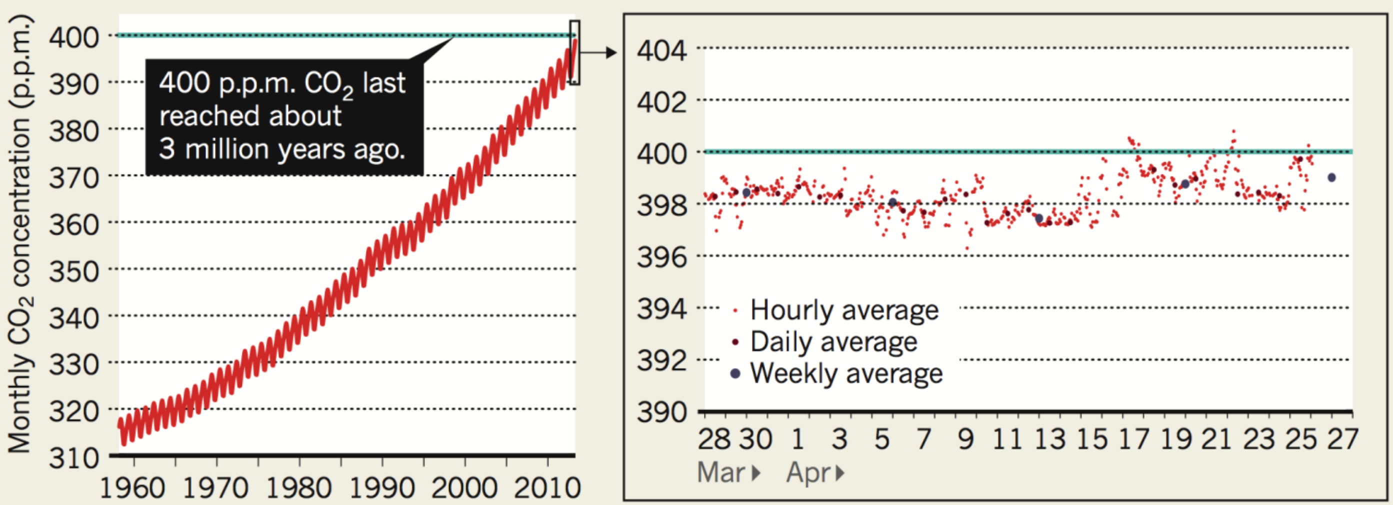

14 | NATURE| VOL497 | 2MAY2013

Multi-scale mitigation efforts

California AB-32

Nature, Dec. 2012


NEWS IN FOCUS

Cities such as Los Angeles produce plumes of pollution that contain greenhouse gases.

CLIMATE CHANGE

Megacities move to track emissions

Scientists monitor greenhouse gases in urban areas as a first step to gauging success of climate initiatives worldwide.

Independent efforts are being made to help mitigate climate change

A changing carbon cycle

A steep road to climate stabilization

Pierre Friedlingstein

The only way to stabilize Earth's climate is to stabilize the concentration of greenhouse gases in the atmosphere, but future changes in the carbon cycle might make this more difficult than has been thought.

Science, 2008

Changes in the physical climate may undermine the ability of the natural carbon cycle to partially sequester atmospheric CO2

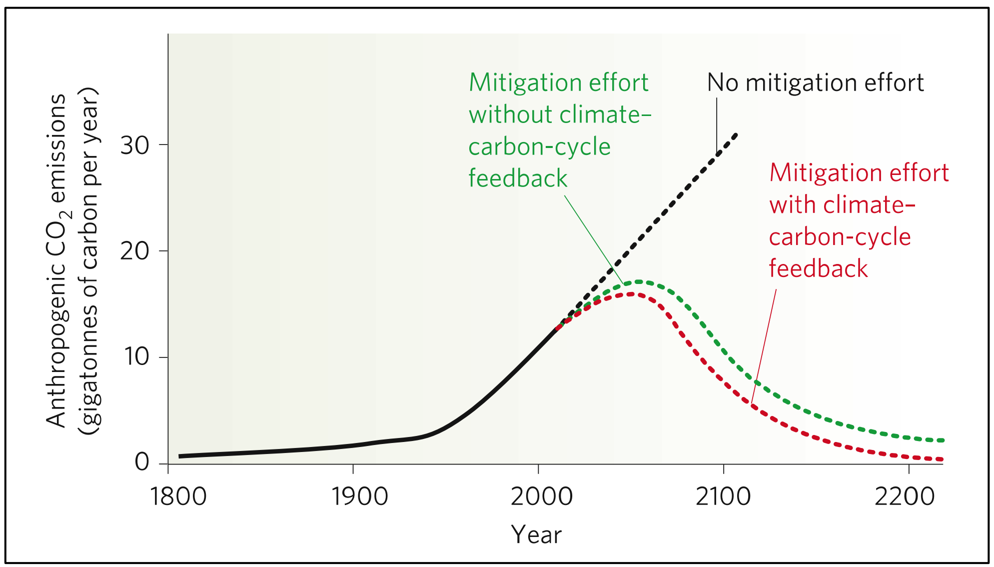

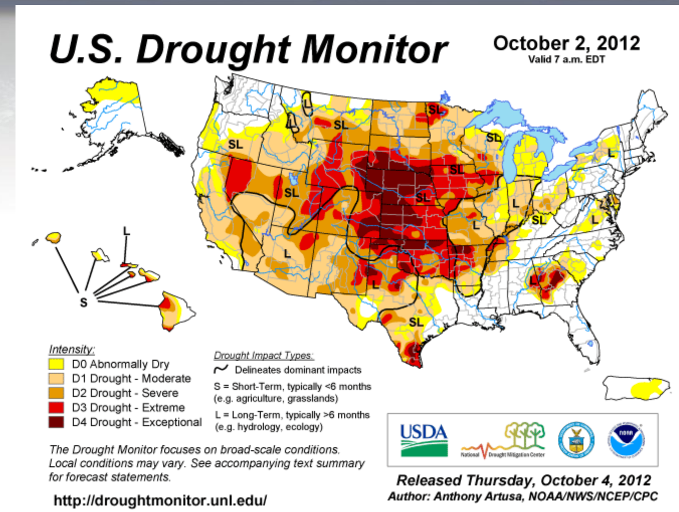

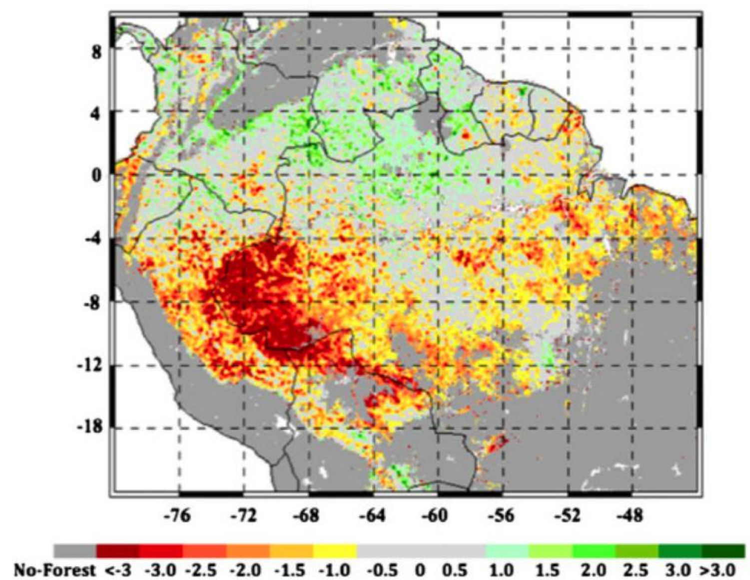

Saatchi *et al*, PNAS, 2013

NASA Carbon Monitoring System

http://carbon.nasa.gov

The objective of the NASA CMS Flux Project is to incorporate the full suite of NASA observational, modeling, and assimilation capabilities to attribute climate forcing to spatially resolved surface fluxes across the entire carbon cycle.

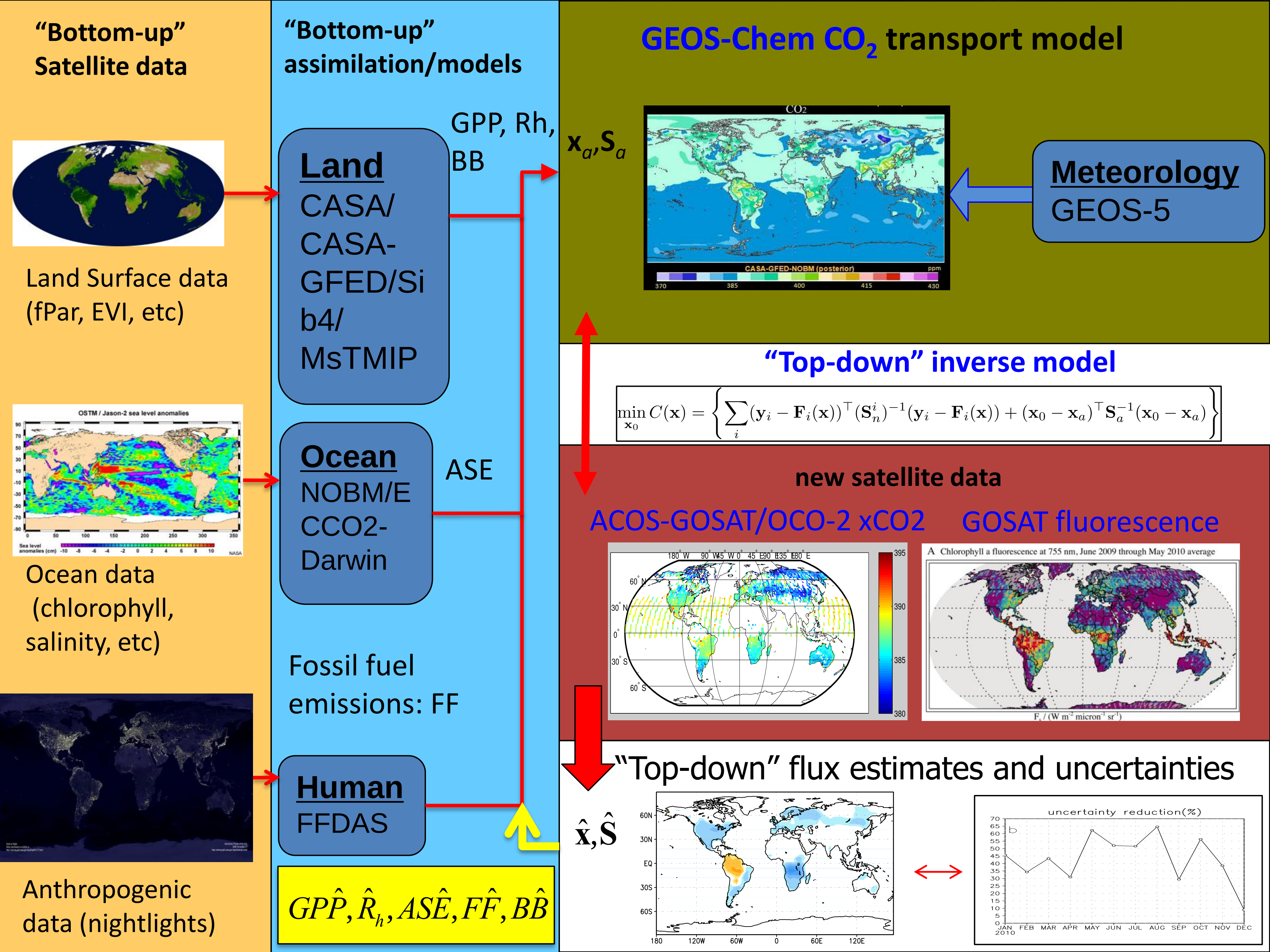

"Bottom-up" Satellite data
"Bottom-up" assimilation/models
GEOS-Chem CO_2 transport model
Land Surface data (fPar, EVI, etc)
Land
CASA/ CASA-GFED/Sib4/ MsTMIP
GPP, Rh, BB
$\mathbf{x}_a, \mathbf{S}_a$
CO2
CASA-GFED-NOBM (posterior)
ppm
370 385 400 415 430
Meteorology
GEOS-5
"Top-down" inverse model
$$\min_{\mathbf{x}_0} C(\mathbf{x}) = \left\{ \sum_i (\mathbf{y}_i - \mathbf{F}_i(\mathbf{x}))^\top (\mathbf{S}_n^i)^{-1} (\mathbf{y}_i - \mathbf{F}_i(\mathbf{x})) + (\mathbf{x}_0 - \mathbf{x}_a)^\top \mathbf{S}_a^{-1} (\mathbf{x}_0 - \mathbf{x}_a) \right\}$$
OSTM / Jason-2 sea level anomalies
Sea level anomalies (cm)
NASA
Ocean data (chlorophyll, salinity, etc)
Ocean
NOBM/ECCO2-Darwin
ASE
new satellite data
ACOS-GOSAT/OCO-2 xCO2
GOSAT fluorescence
A Chlorophyll a fluorescence at 755 nm, June 2009 through May 2010 average
F_s / (W m^{-2} micron^{-1} sr^{-1})
Fossil fuel emissions: FF
Human
FFDAS
Anthropogenic data (nightlights)
"Top-down" flux estimates and uncertainties
$\hat{\mathbf{x}}, \hat{\mathbf{S}}$
uncertainty reduction(%)
JAN 2010 FEB MAR APR MAY JUN JUL AUG SEP OCT NOV DEC
$G\hat{PP}, \hat{R}_h, AS\hat{E}, F\hat{F}, B\hat{B}$

Observations of xCO2 from space-

The NASA Orbiting Carbon Observatory-2 (OCO-2) and JAXA-GOSAT Mission

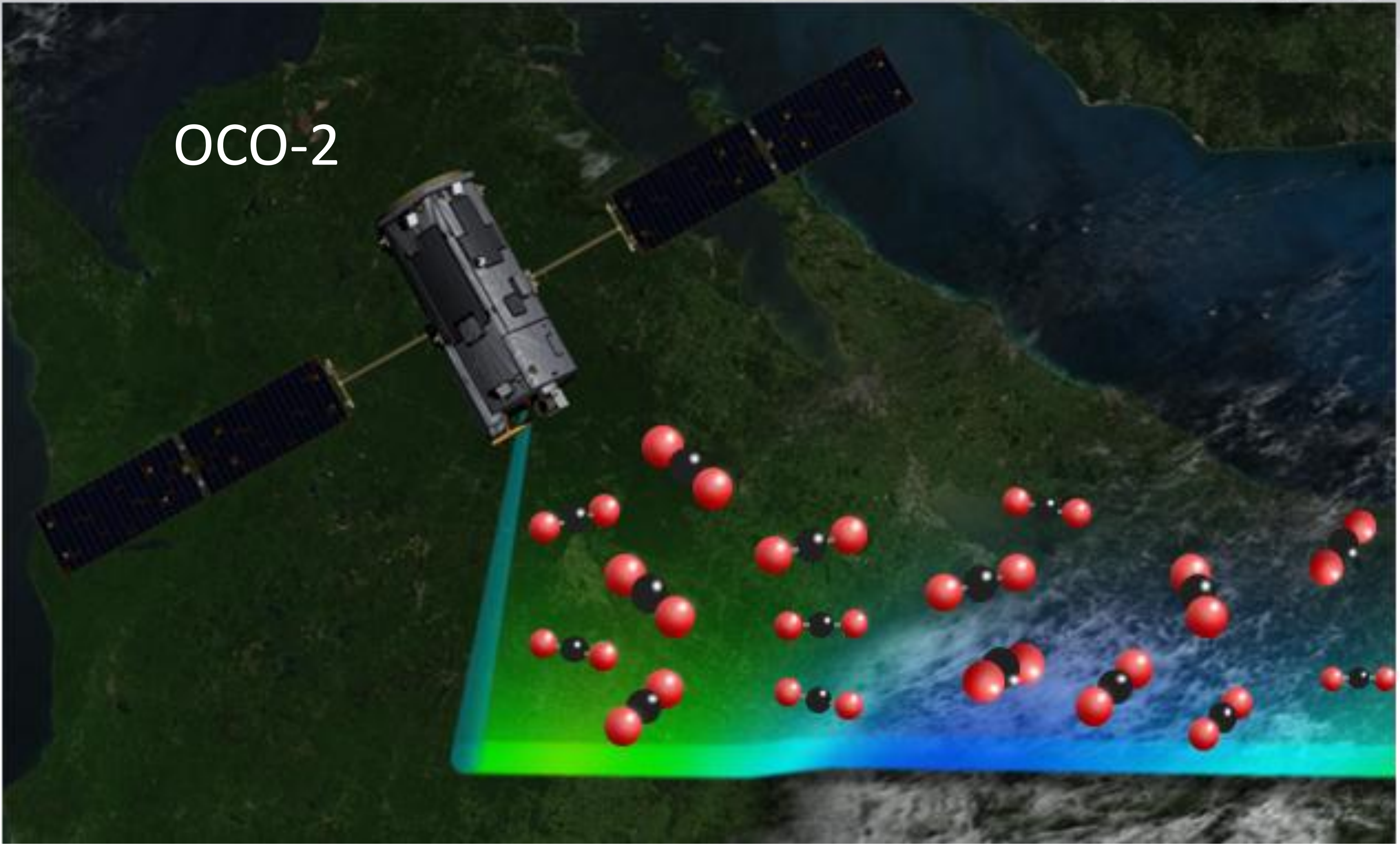

Measuring CO_2 from Space

- **Record** spectra of CO_2 and O_2 absorption in reflected sunlight

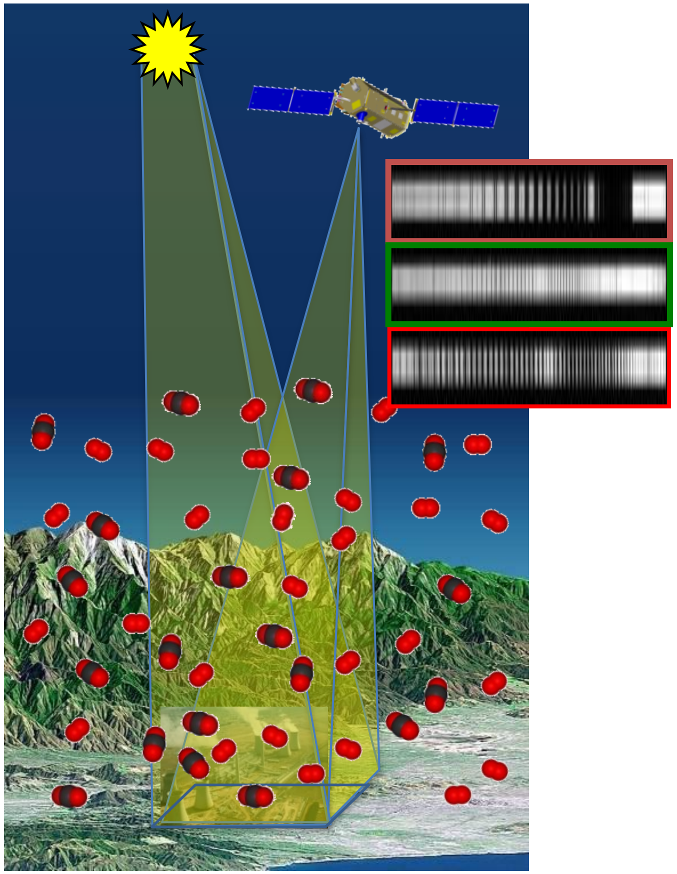

- **Retrieve** variations in the *column averaged CO_2 dry air mole fraction, X_{CO2}* over the sunlit hemisphere

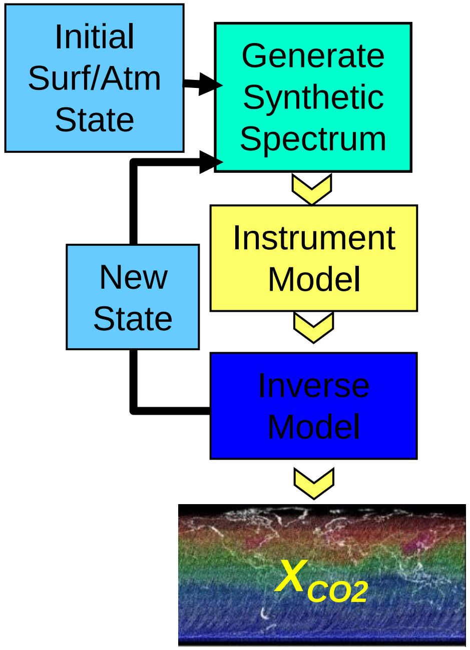

- **Validate** measurements to ensure X_{CO2} accuracy of 1 - 2 ppm (0.3 - 0.5%)

Courtesy David Crisp, JPL

Attribution Strategy

A priori carbon cycle budgets are constructed to be consistent with atmospheric CO2 growth

10.1 GtC ± 0.5 GtC

5.0 ± 0.2 PgC y^{-1}

50%

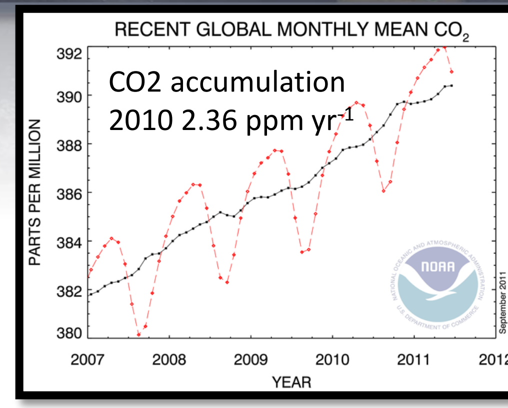

2.6 ± 1.0 PgC y^{-1}

26%

Calculated as the residual of all other flux components

Fossil Fuel+Land Use Change (CDIAC+Global Carbon Project 2010)
Incorporates chemical CO2 production aviation, bunker, and shipping (Nassar et al, 2010)

24%

2.4 ± 0.5 PgC y^{-1}

Derived from ECCO-2 ocean flux estimate

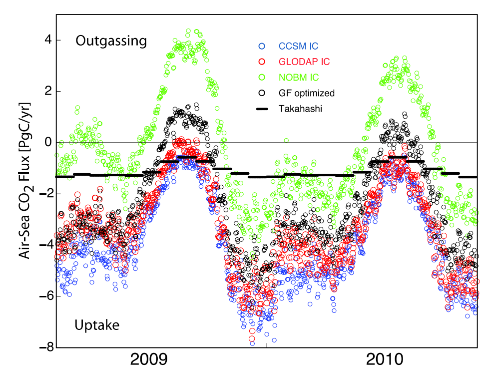

4D-var assimilation approach

$$\min_{\mathbf{x}_0} C(\mathbf{x}) = \left\{ \sum_i (\mathbf{y}_i - \mathbf{F}_i(\mathbf{x}))^\top (\mathbf{S}_n^i)^{-1} (\mathbf{y}_i - \mathbf{F}_i(\mathbf{x})) + (\mathbf{x}_0 - \mathbf{x}_a)^\top \mathbf{S}_a^{-1} (\mathbf{x}_0 - \mathbf{x}_a) \right\}$$

$$\text{subject to } \mathbf{x}_{i+1} = \mathbf{M}_i(\mathbf{x}_i, \mathbf{p}_i)$$

State vector $\mathbf{x} = \begin{bmatrix} \mathbf{q} \\ \mathbf{e} \end{bmatrix}$

Initial conditions

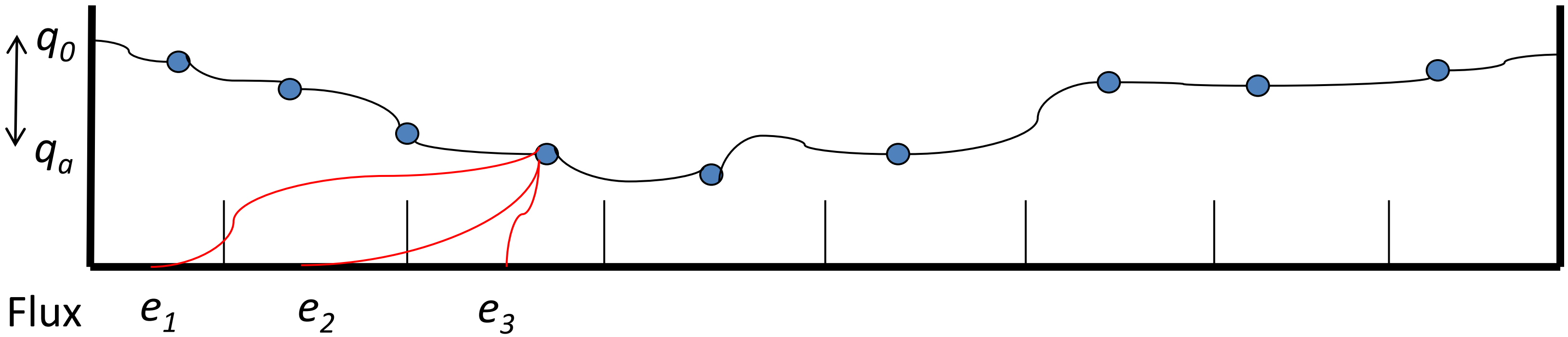

- Both an initial condition and boundary condition problem
- Initial conditions solved through "sliding window" technique from Feng and Jones (UT)
- Monthly NEE estimated over a year window.
- Estimate of terrestrial flux **only**

4D-var
x: monthly scale factor
$[\mathbf{S}_a]_{ii}$ = CASA-GFED3 Monte Carlo
$\mathbf{S}_n$ = Observational error from ACOS. No transport error or horizontal correlation error.

CASA-GFED3 terrestrial eco-system model

- The CASA-GFED3 model is modified to have an annual flux consistent with the inferred terrestrial flux.
- Spatial uncertainties are estimated through a Monte Carlo analysis through perturbation of key environmental parameters such as maximum potential light use efficiency, Q10, forest tree cover, etc.
    - Quantifies parameteric uncertainty (but not structural uncertainty)

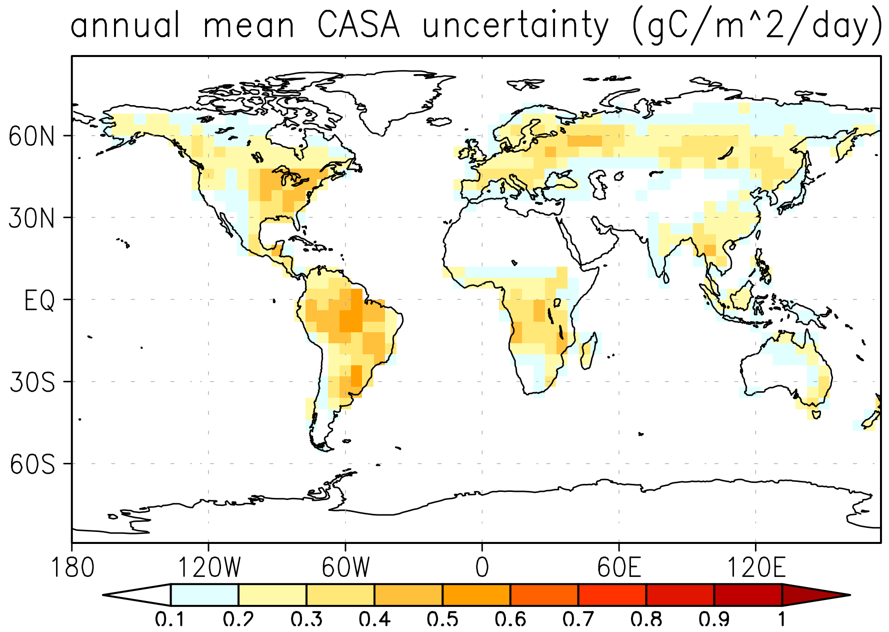

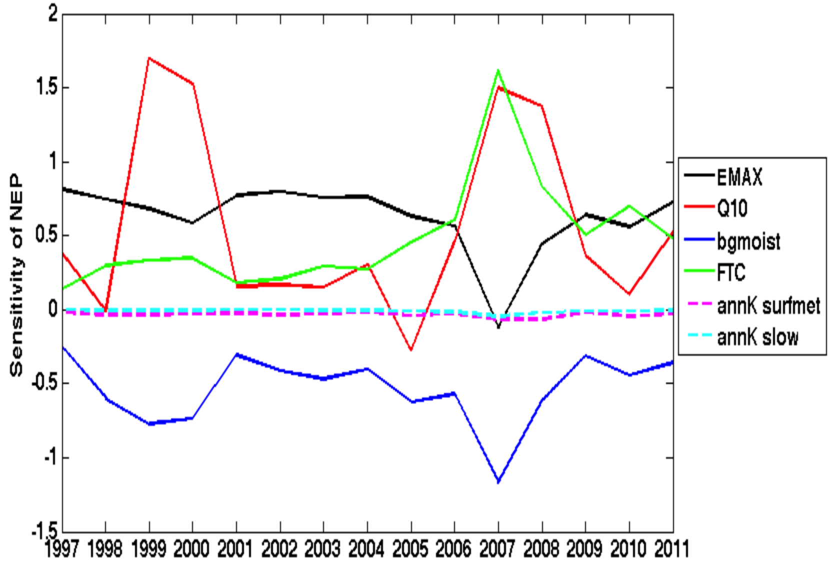

Interannual sensitivity of global *NEP* (no fire) to selected CASA-GFED parameters.

CASA-GFED NEE uncertainty: role of the tropics

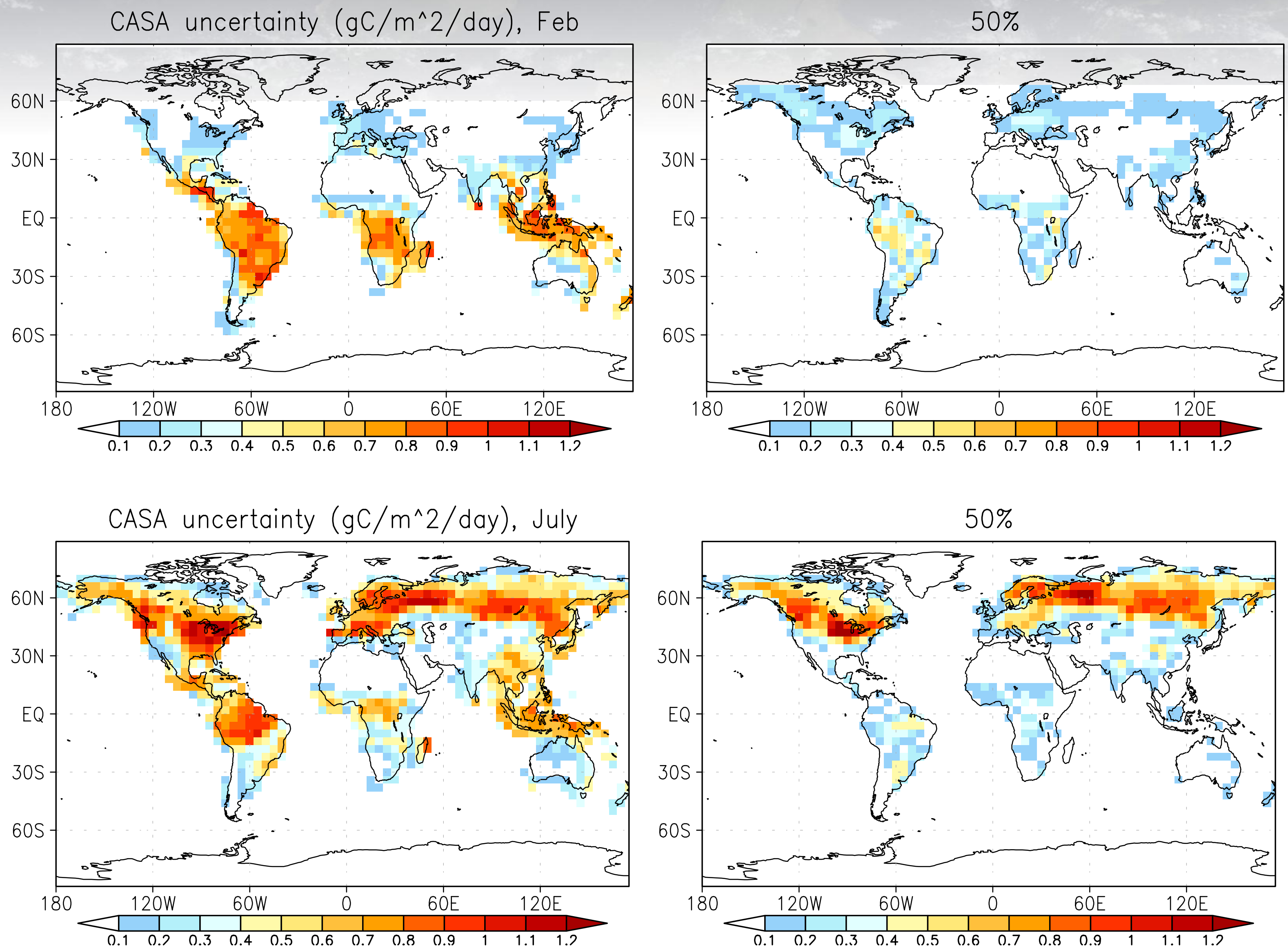

ECCO2-Darwin ocean biogeochemical model

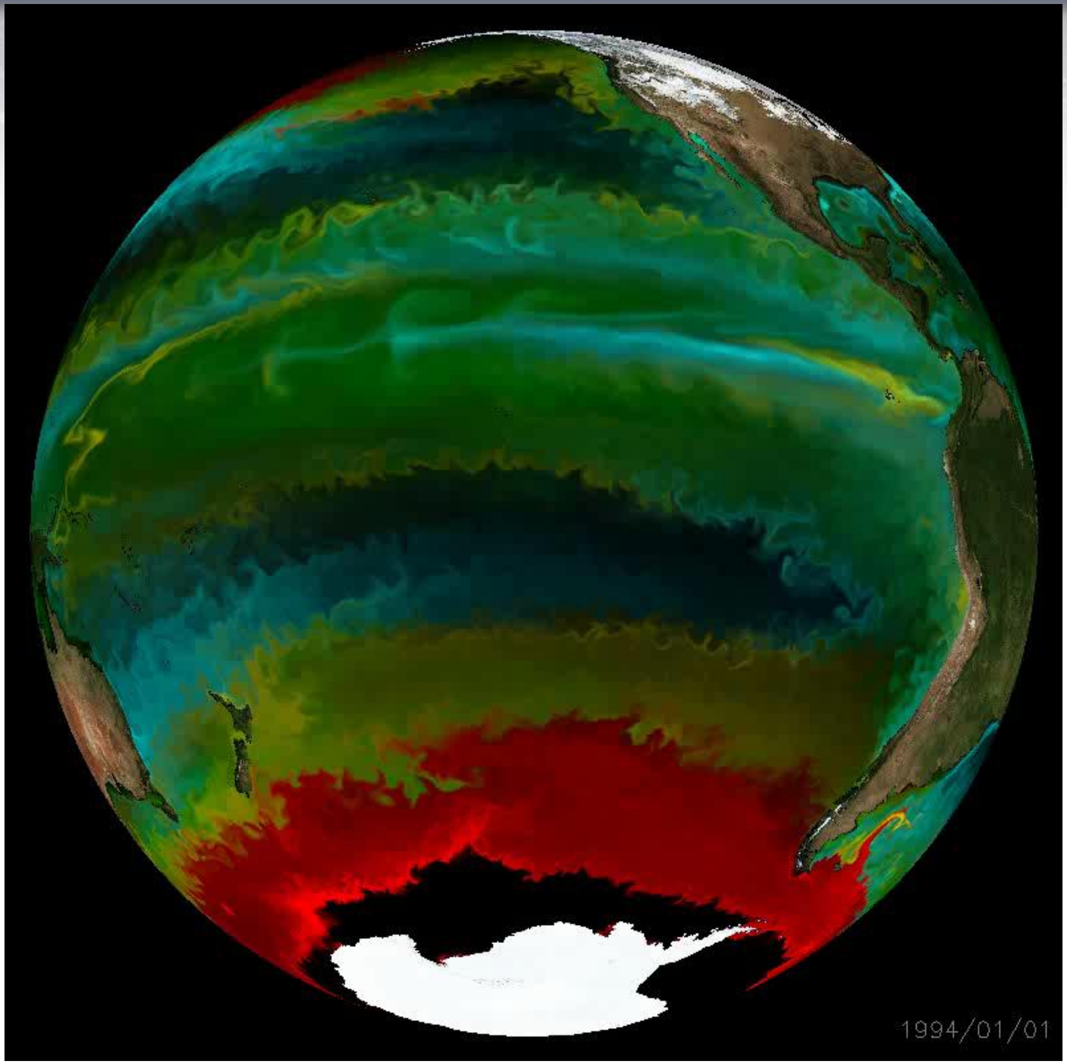

Concentration of different species categories
Diatoms (red), Prochlorococus (green)
Picoplankton (blue), Everything else (yellow)

ECCO2: Eddying Global-Ocean and Sea-Ice Data Synthesis
18 km-cubed sphere, physical ocean 4D---variational assimilation
(Menemenlis et al, 2008)
Darwin: Ocean Biogeochemistry (Follows et al., 2007)

Biogeochemistry is constrained by a Green's function approach (least squares)

Model: $\boldsymbol{y} - G\,[\mathbf{x}_b] \approx \mathbf{G}\,(\mathbf{x} - \mathbf{x}_b) + \mathbf{n}$

Solution:

$$\mathbf{x} = \mathbf{x}_b + (\mathbf{G}^T\mathbf{G})^{-1}\,\mathbf{G}^T\,(\boldsymbol{y} - G\,[\mathbf{x}_b])$$

G is a kernel matrix whose columns are computed using a GCM sensitivity experiment for each parameter in vector **x**, which are the initial conditions. Subscript "b" represents baseline GCM integration used to linearize problem.

Preliminary assimilation of LDEO pCO2, 2009-2010

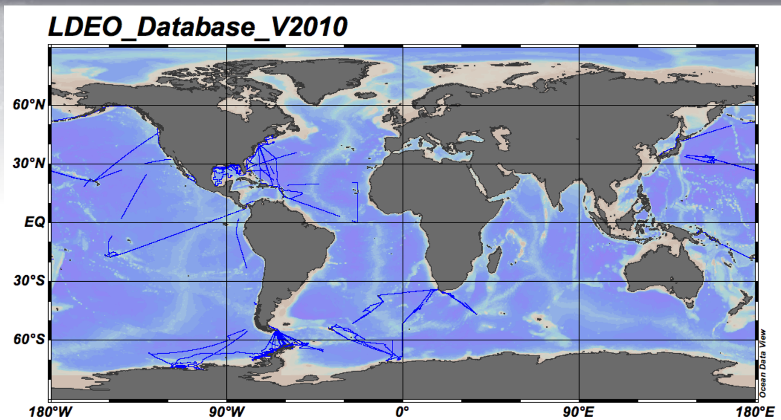

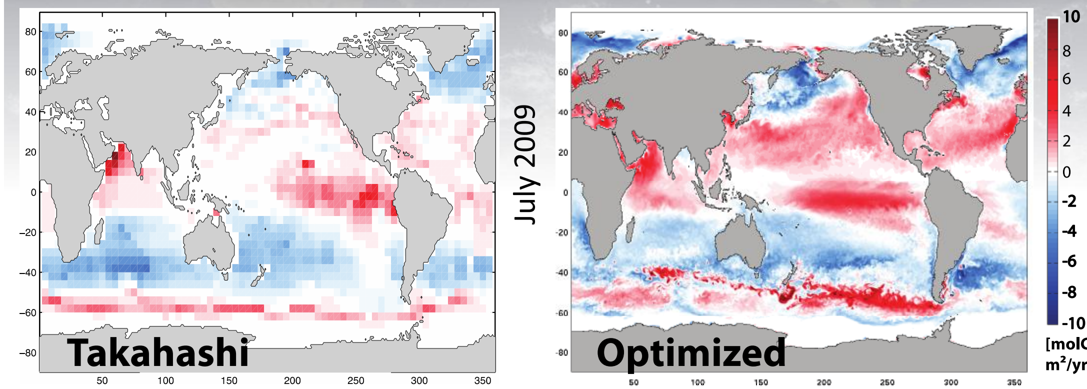

Seven ECCO2-Darwin sensitivity integrations differing in their initial conditions (IC) for dissolved inorganic carbon (DIC), alkalinity (Alk), and oxygen and in biogeochemical parameterizations were used for the optimization.

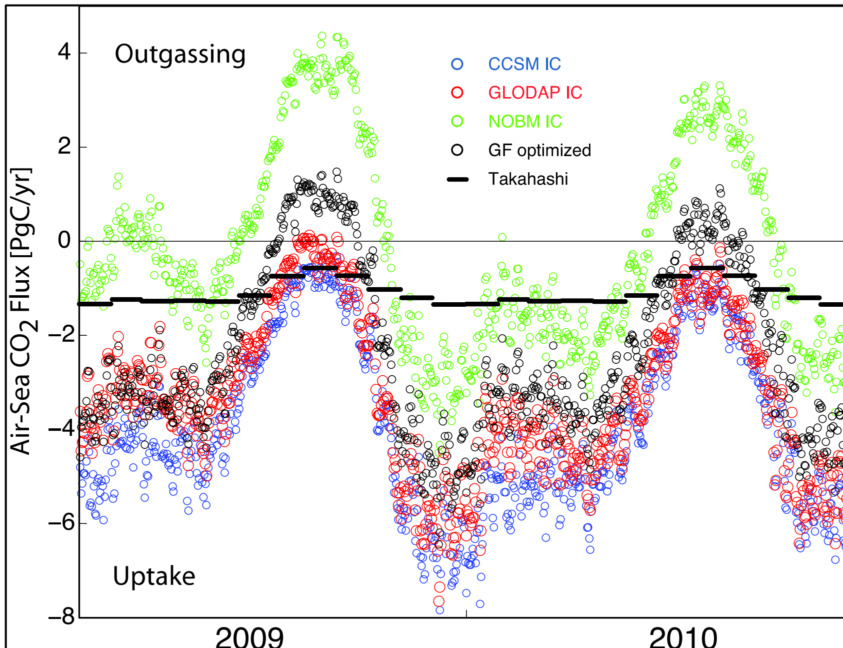

Simulated mean air-sea CO_2 fluxes during 2009-2010 in PgC/yr:

NOBM IC: -0.2

Takahashi: -1.1

Optimized: -2.4

GLODAP IC: -3.5

CCSM IC: -4.0

Brix *et al,* in preparation (2013)

Comparison of CMS-Flux to GOSAT

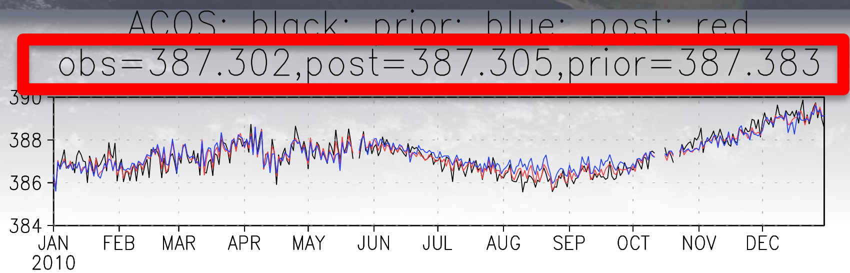

- CMS-Flux total annual flux agrees with GOSAT to within 0.01 ppm.
- Zonal and seasonal differences range from 0.5 to 1 ppm

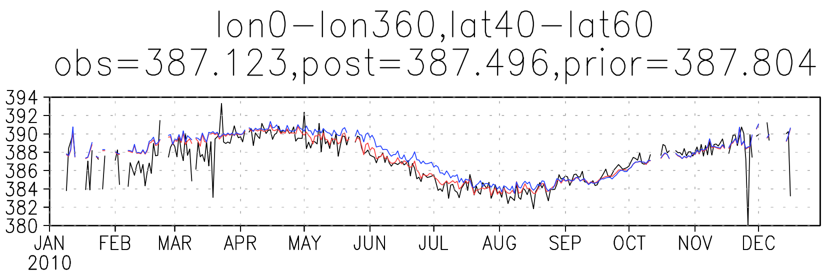

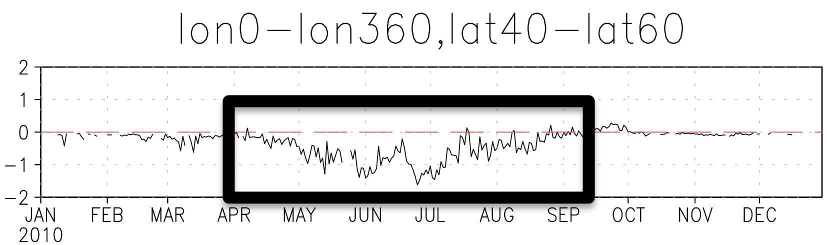

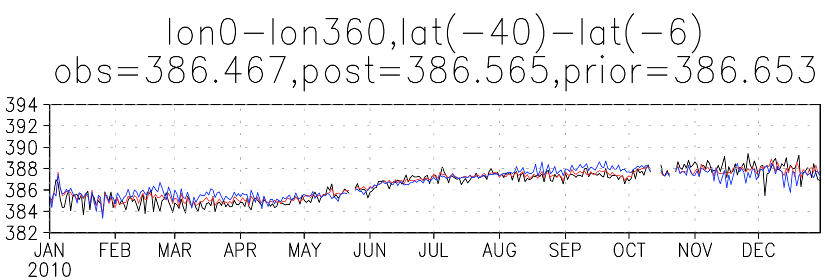

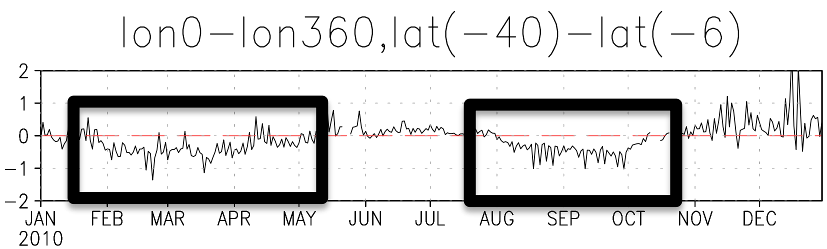

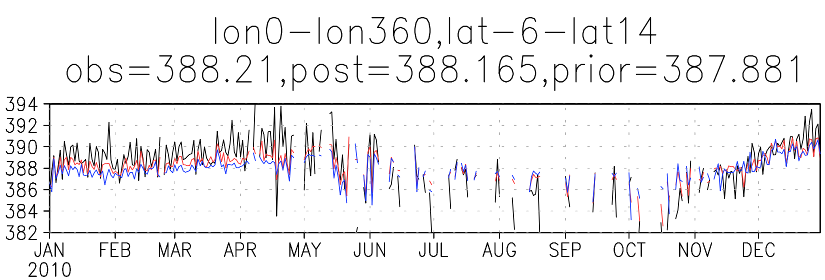

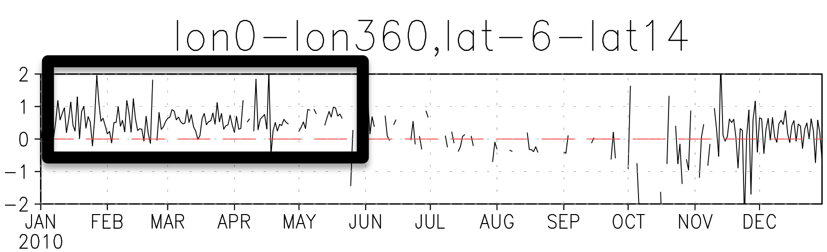

Posterior flux estimate 2010

Prior flux=-5.12GtC, posterior flux=-5.36GtC

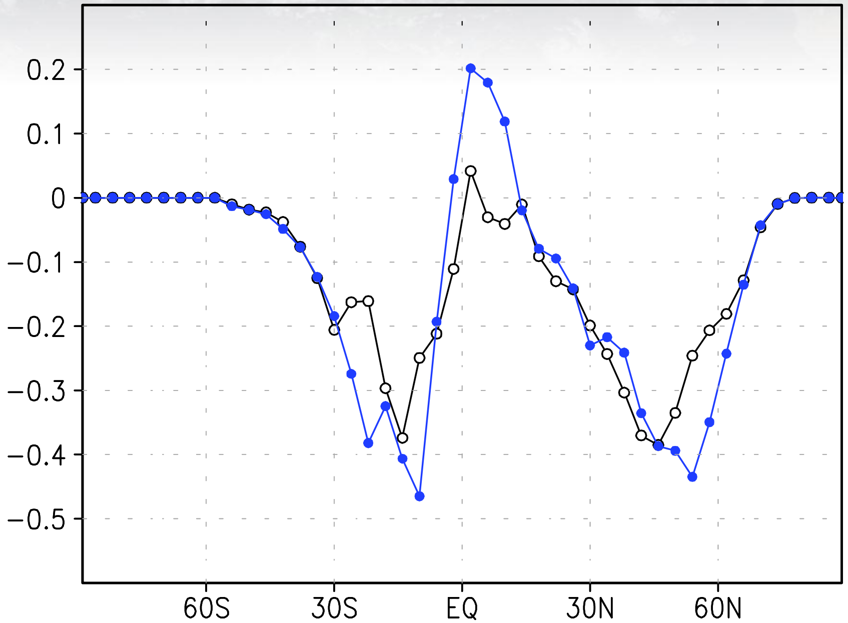

Black: prior; blue: posterior; green: fossil fuel; red: biomass burning; purple: ocean flux

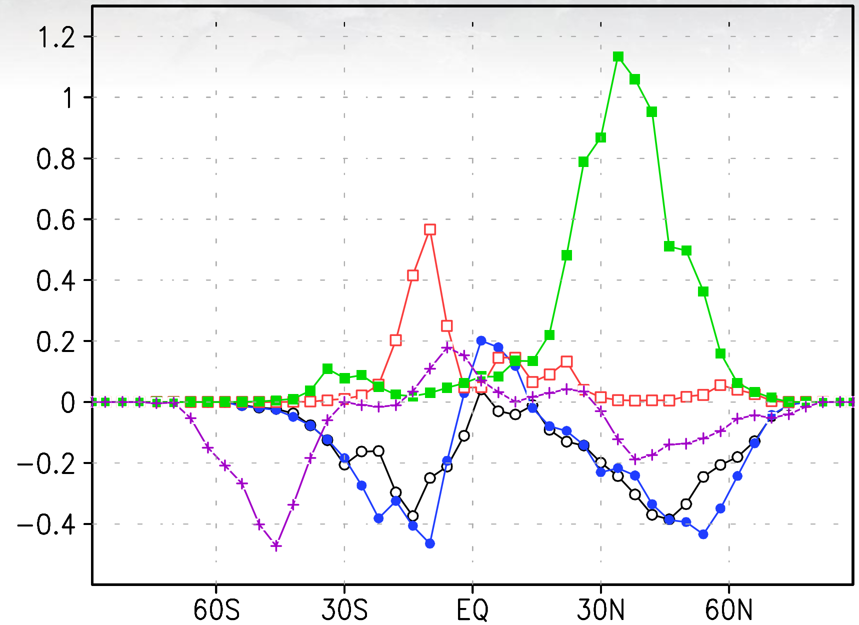

- Prior flux (Black); Posterior flux (blue)
- Posterior estimate redistributes the flux merdionally.
- The posterior flux increases carbon uptake over the NH mid-latitude and SH sup-tropics while reducing uptake over the tropics relative to the prior carbon budget.
- It's important to remember that xCO2 is only sensitivity to the total flux. Uncertainties in one part of the carbon cycle can alias into the other.

Spatial attribution of CO_2

Annual mean prior flux ($gC/m^2/day$)

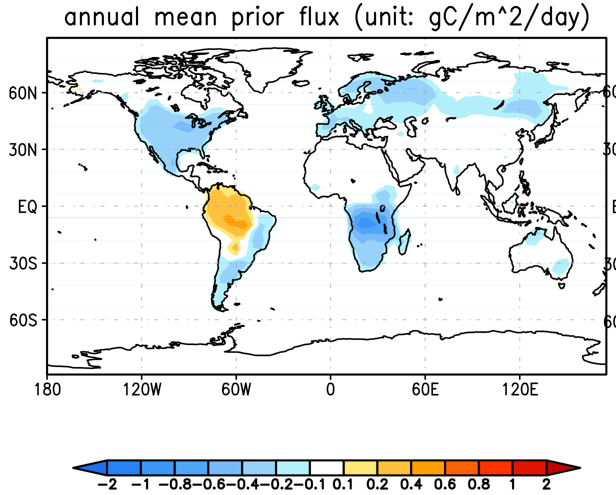

Annual mean posterior flux ($gC/m^2/day$)

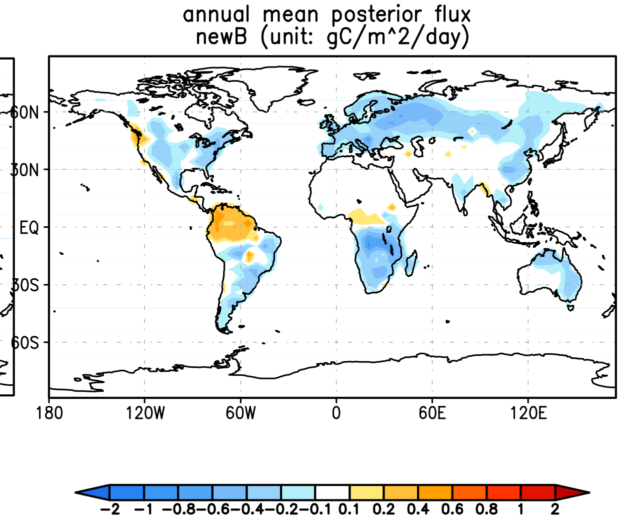

Post-prior ($gC/m^2/day$)

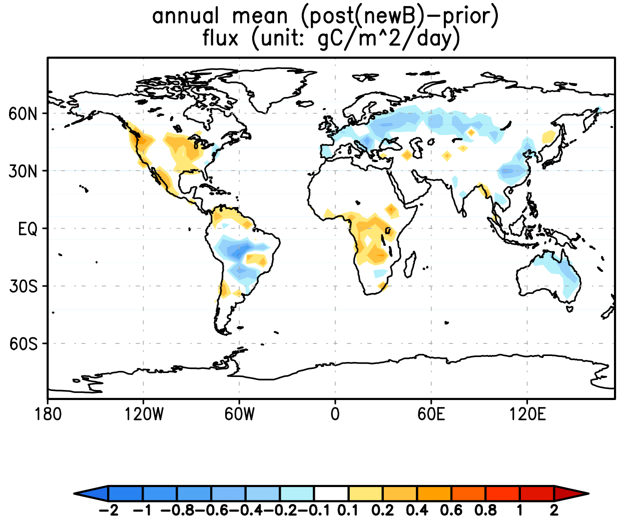

- Zonal redistribution of carbon uptake in the Northern Hemisphere between Europe (stronger) and North America (weaker)
- Zonal redistribution in the tropics with reduced uptake in Africa but increased uptake in the Amazon

Anthropogenic emissions and Biomass burning

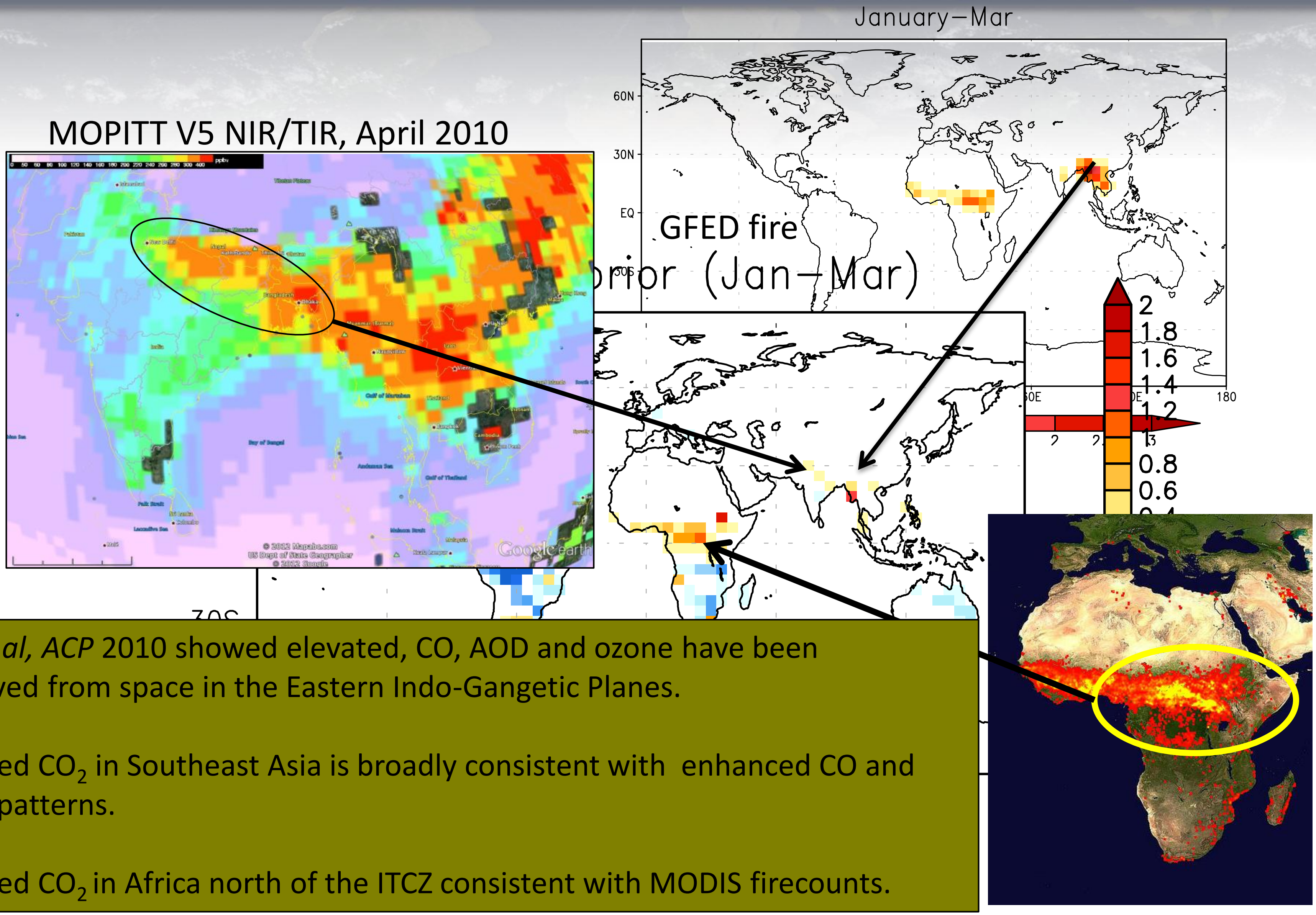

Kar *et al, ACP* 2010 showed elevated, CO, AOD and ozone have been observed from space in the Eastern Indo-Gangetic Planes.

Elevated CO_2 in Southeast Asia is broadly consistent with enhanced CO and GFED patterns.

Elevated CO_2 in Africa north of the ITCZ consistent with MODIS firecounts.

European sink and African biomass burning

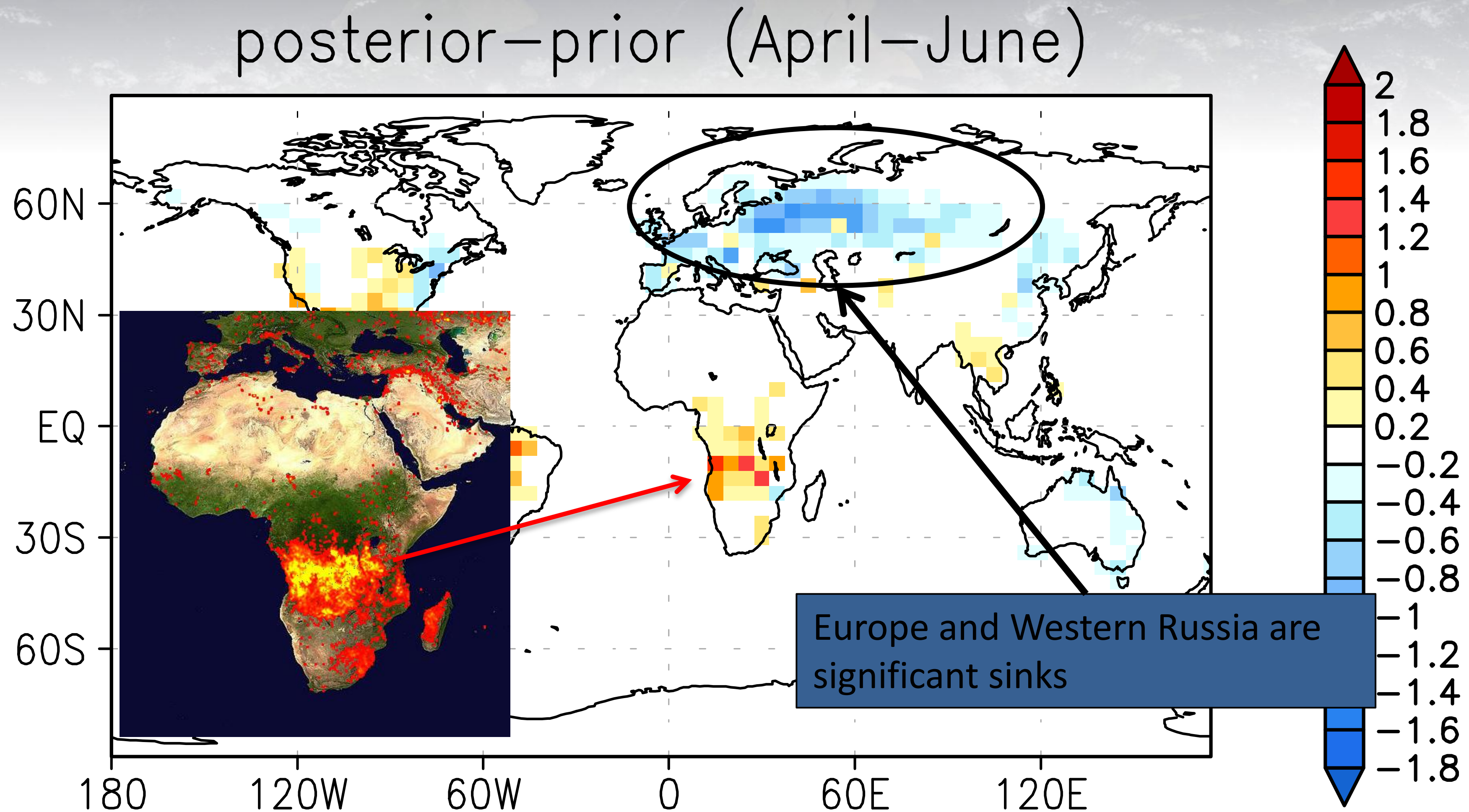

Impact of spatial sampling

y-H(x_a) (prior flux)

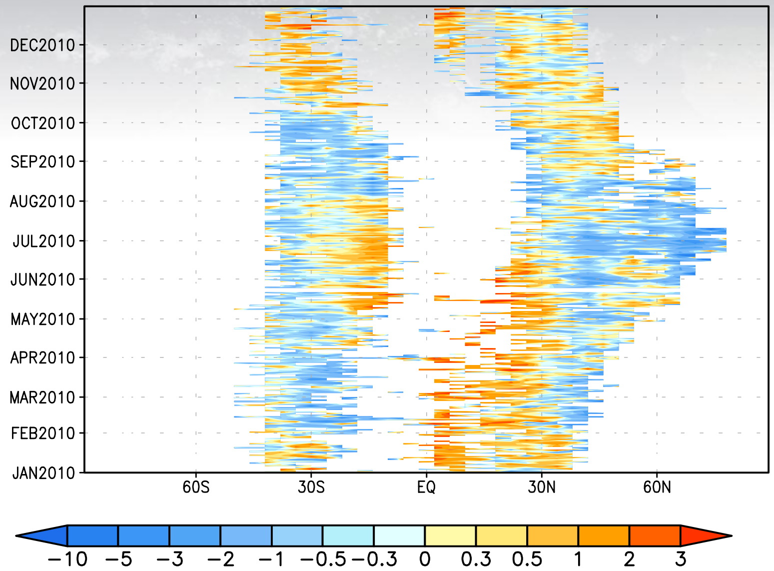

y-H(x’) (posterior flux)

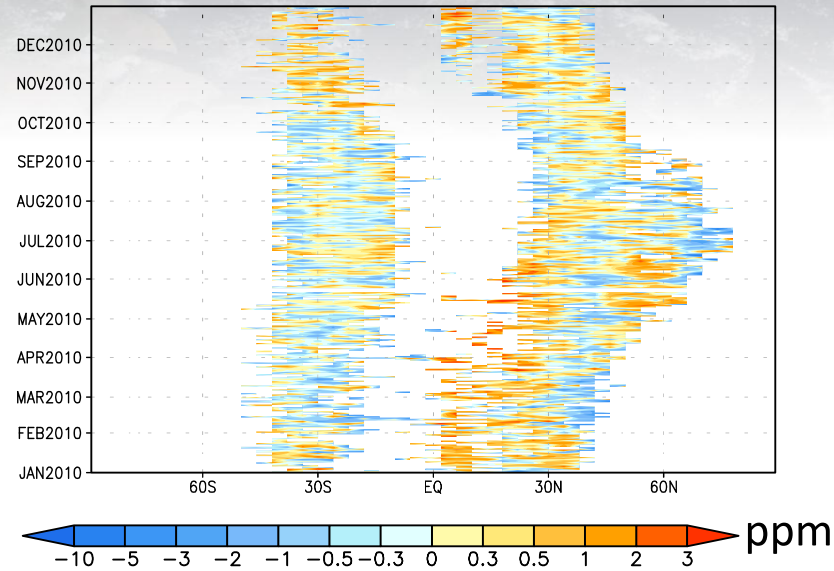

- Residual difference (obs-model) shows a strong meridional shift during NH summer.
- Tropical sampling driven by the ITCZ
- Large parts of the world are not observed
  - Southern Hemisphere
  - Northern Hemisphere during Winter and Fall
- Mean residual difference markedly reduced over the year.
- Pattern of differences largely the same
  - Over correcting at mid-high latitudes in the NH during summer time;

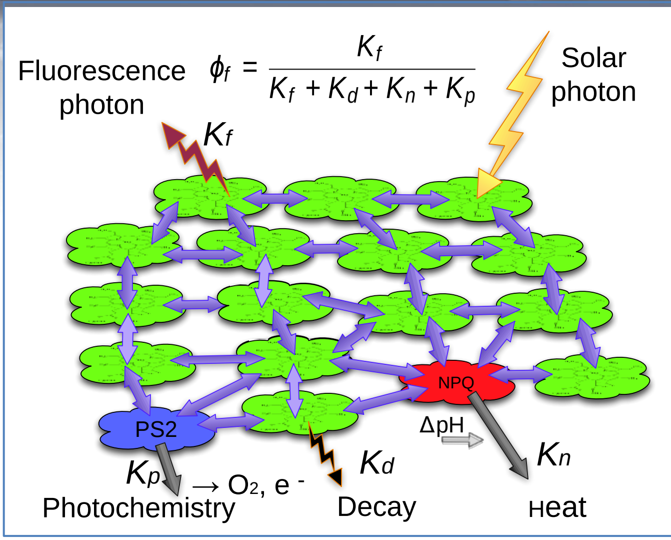

Solar induced Chlorophyll Fluorescence (SIF) is a direct by-product of photosynthesis → unique dynamic proxy for gross primary production GPP.

$$SIF = PAR \cdot fPAR \cdot \phi_f$$

$$GPP = SIF \cdot \phi_p / \phi_f$$

New Methods for Measurements of Photosynthesis from Space!

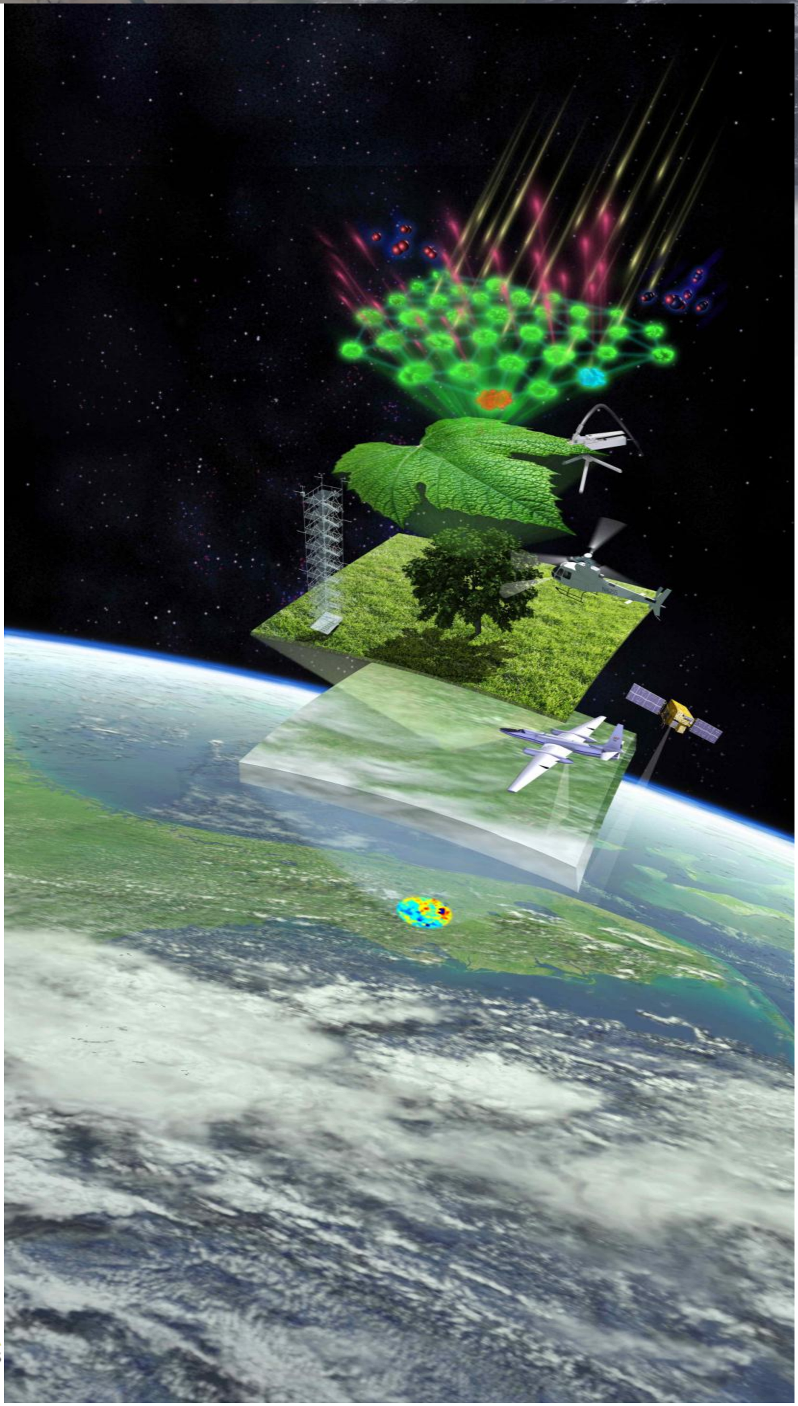

Planetary photosynthesis

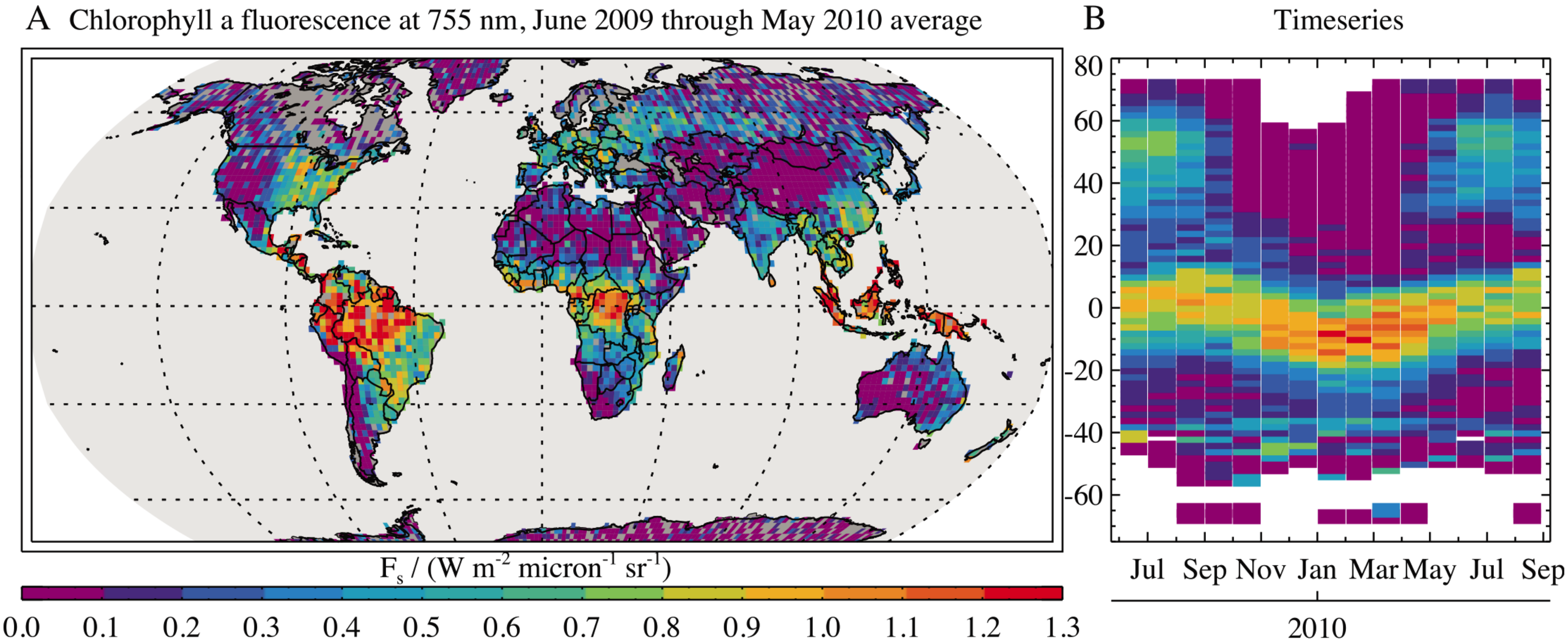

Figure 1. (a) Annual average (June 2009 through May 2010) of retrieved chlorophyll-a fluorescence at 755 nm on a 2° × 2° grid. Only grid-boxes with more than 15 soundings constituting the average are displayed. (b) Latitudinal monthly averages of chlorophyll fluorescence from June 2009 through end of August 2010.

Frankenberg *et al*, 2011

Fluorescence can be measured from GOSAT, GOME-2, and soon OCO-2

Covariation with GPP

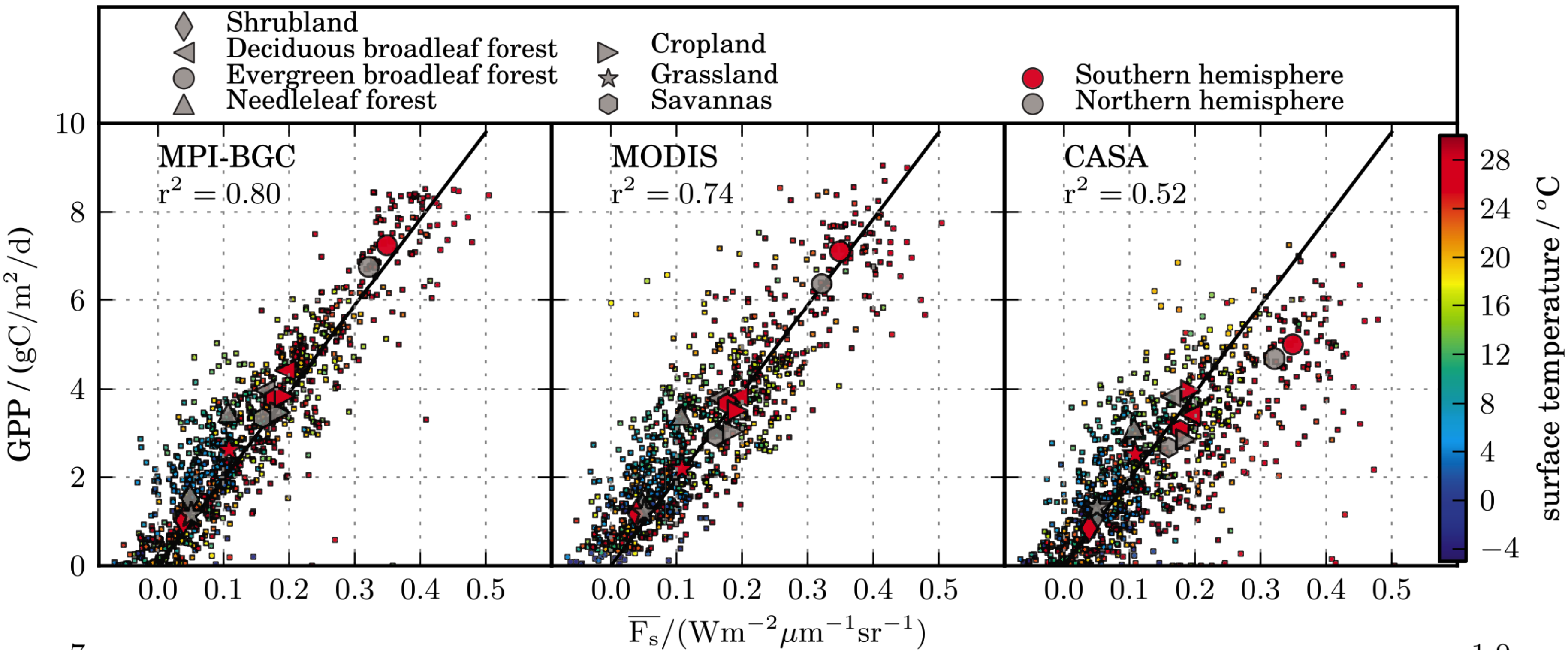

Frankenberg *et al*, 2011

Comparisons with MPI-BGC point to the proportionality of GPP to fluorescence.

Constraints on GPP from SIF

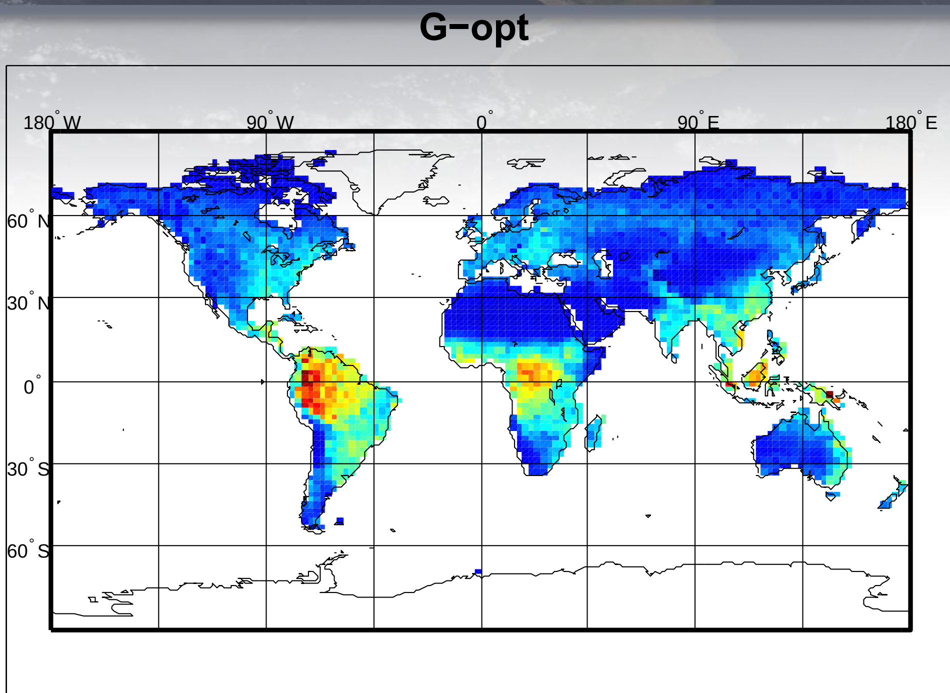

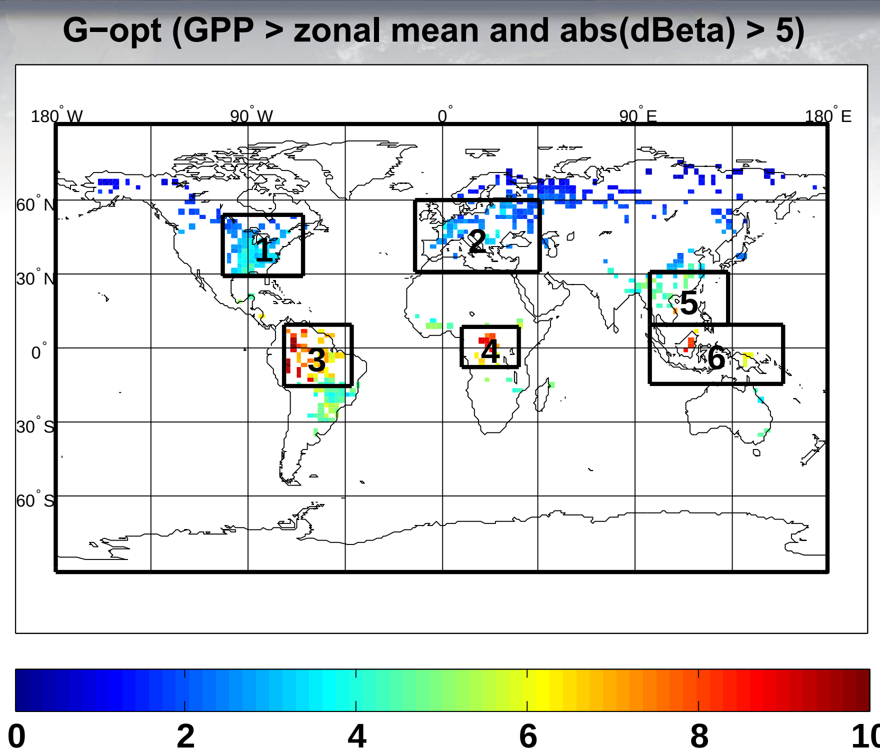

gC/m^2/day

Parazoo et al, *in preparation*

$$\min_{\mathbf{x}_0} C(\mathbf{x}) = \left\{ (\mathbf{y} - \mathbf{F}(\mathbf{x}))^\top \mathbf{S}_n^{-1} (\mathbf{y} - \mathbf{F}(\mathbf{x})) + (\mathbf{x} - \mathbf{x}_a)^\top \mathbf{S}_a^{-1} (\mathbf{x} - \mathbf{x}_a) \right\}$$

- Prior distribution from the TRENDY Models
- Accounts for GOSAT sampling, clouds cover, and precision
- Regions with high error reduction relative to inter-model spread also have high GPP

Connecting GPP to NEE

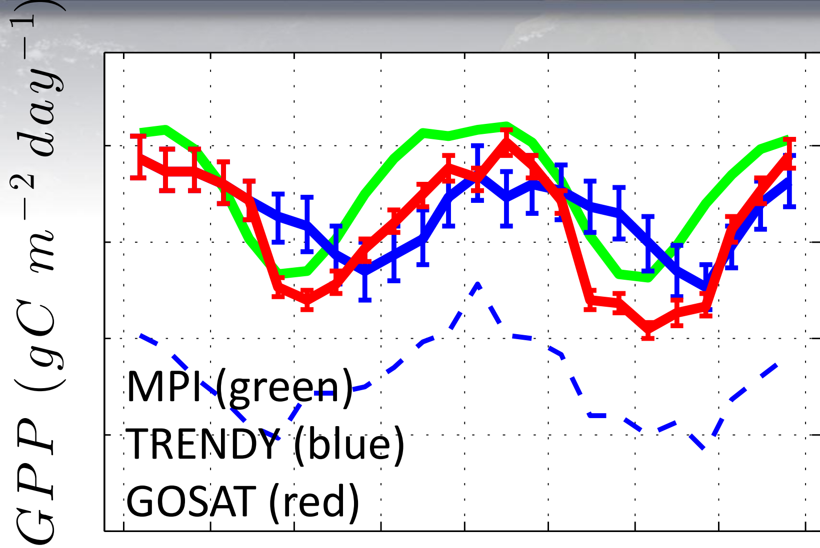

Parazoo et al, GRL 2013

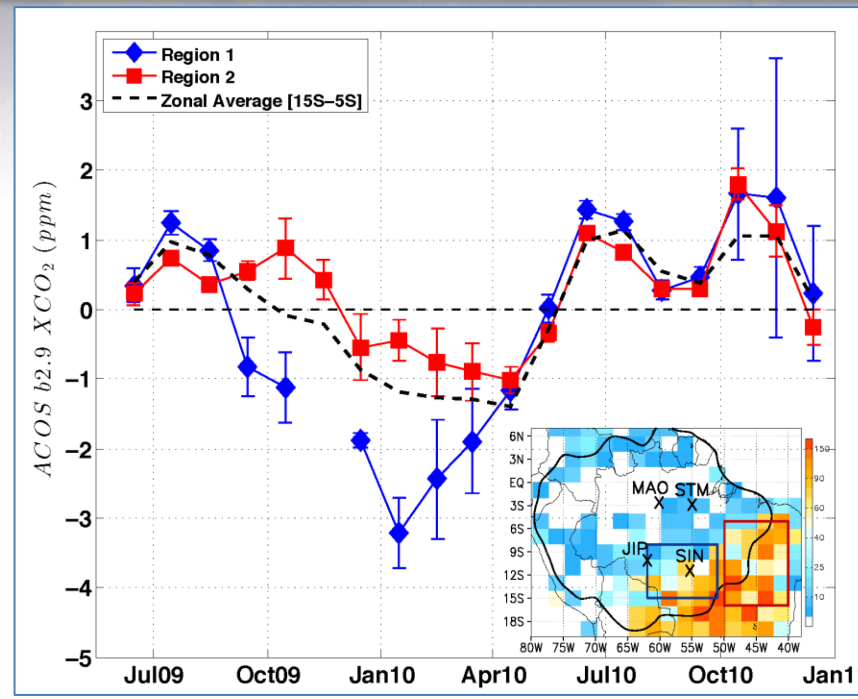

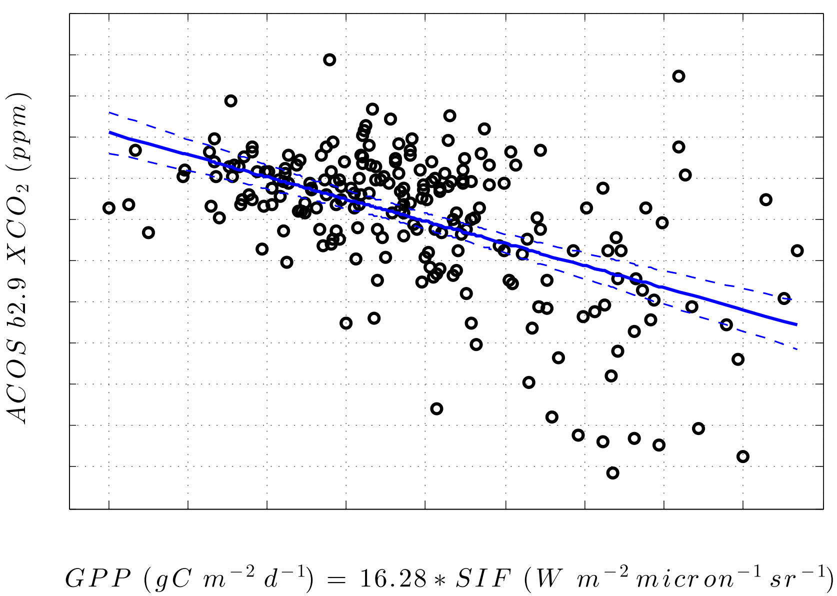

GPP estimates from GOSAT has an earlier draw down in July 2009 and a dramatically weaker GPP in July 2010 than TRENDY

Significant differences in the seasonal cycle of xCO_2 between the tropical transitional forests (TTF) and the cerrado eco-system

Local GPP can explain a significant fraction of xCO_2 variability in TTF

Conclusions

- Quantifying the spatial drivers of climate forcing requires an integrated approach of data, model, and assimilation across the entire carbon cycle.
- Preliminary estimates indicate large-scale zonal and meridional redistribution of carbon uptake relative to the a prior carbon budget
  - Tropical changes appear to be related to biomass burning
  - Northern hemispheric redistribution is potentially related to GOSAT sampling
- The combination of fluorescence-derived GPP and eco-system model estimates show significant variations in sensitive eco-system regions.
- The combination of xCO2 and fluorescence shows that the CO_2 seasonal cycle in the tropical transitional forests are strongly influence by local GPP.
- CMS in the context of carbon-climate
  - The CMS is a carbon cycle reanalysis system that can benchmark CMIP5/CMIP6 carbon-climate models.
  - CMS with new satellites: OCO-2, OCO-3, SMAP, BIOMASS, etc. could provide the required sensitivity to detect and attribute the onset of carbon-climate feedbacks
  - Patterns of flux response diagnosed from CMS to patterns of environmental forcing will provide a powerful resource for finding emergent relationships between present day bias and future response.
- More information at http://carbon.nasa.gov and http://cmsflux.jpl.nasa.gov

BACKUP

Comparison to surface data

(red: posterior; blue: prior, black: obs)

Centro de Investigacion de la Baja Atmosfera, Spain

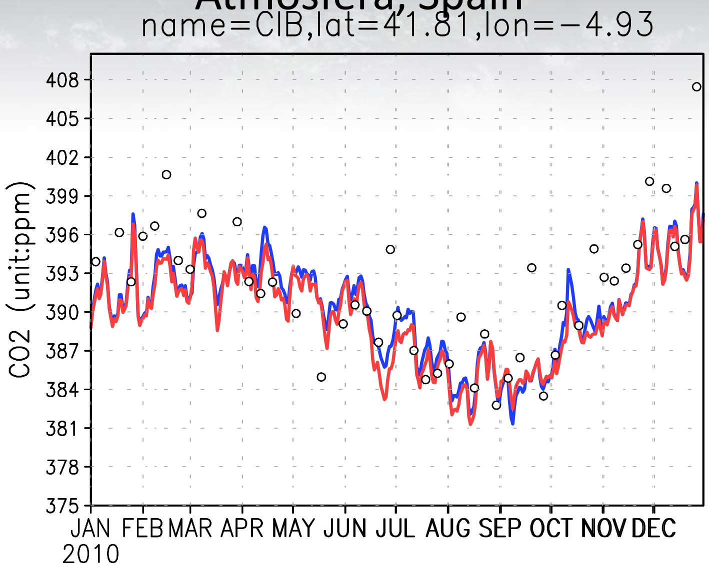

South Pole, Antarctica, US

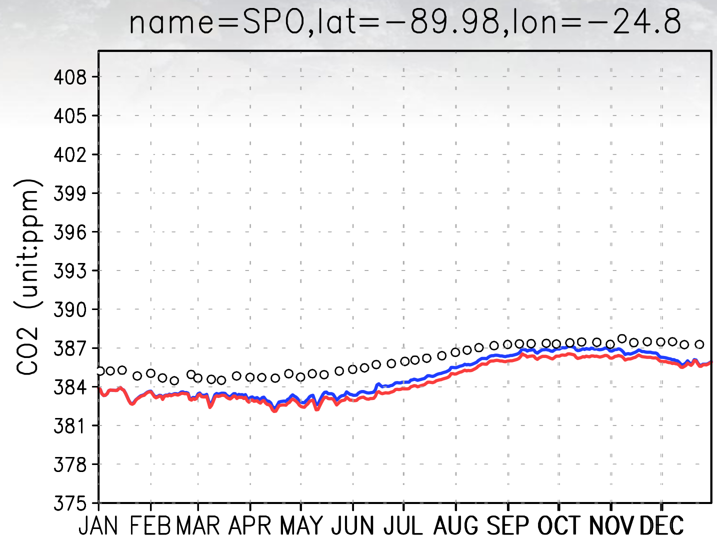

Posterior - prior

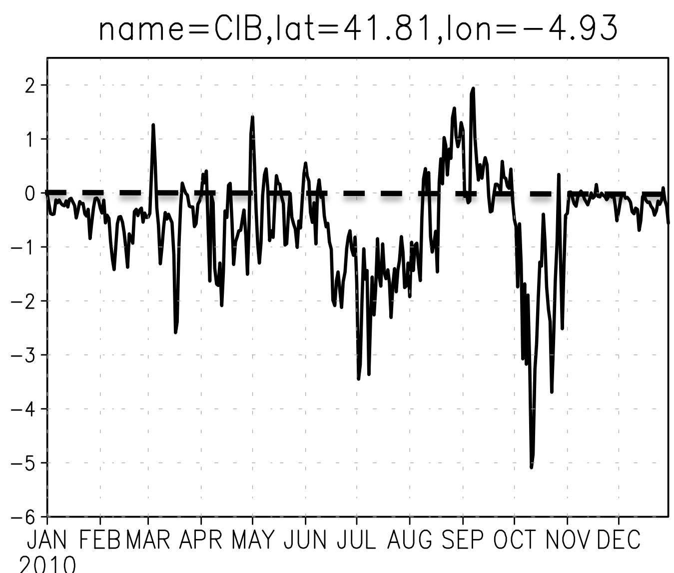

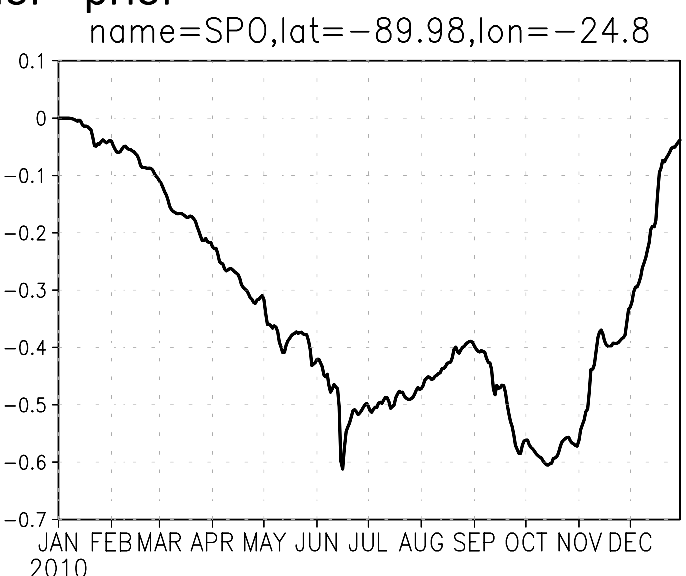

Comparison to surface data

Baring Head Station, New Zealand,

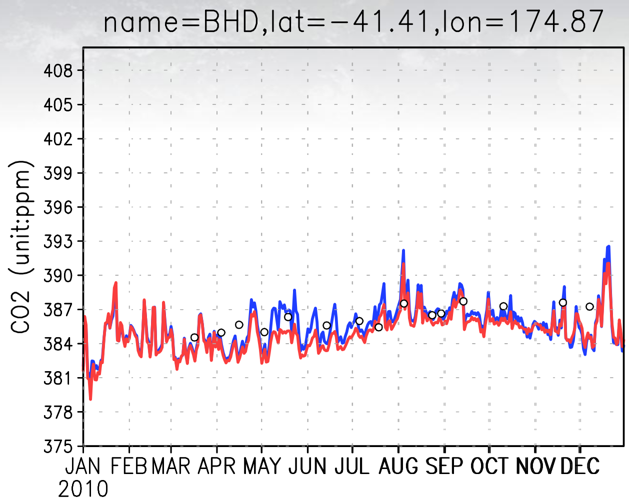

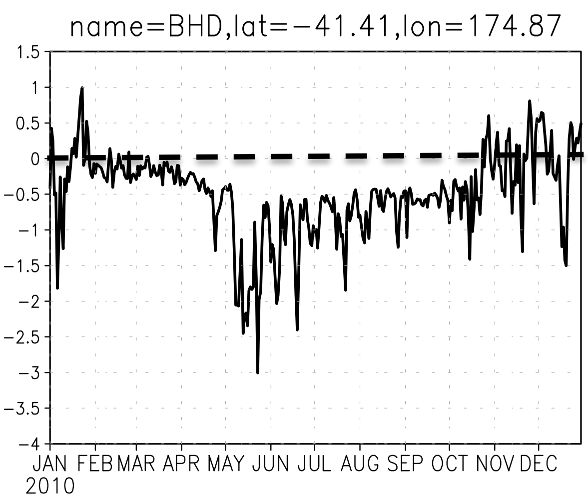

Bukit Kototabang, Indonesia

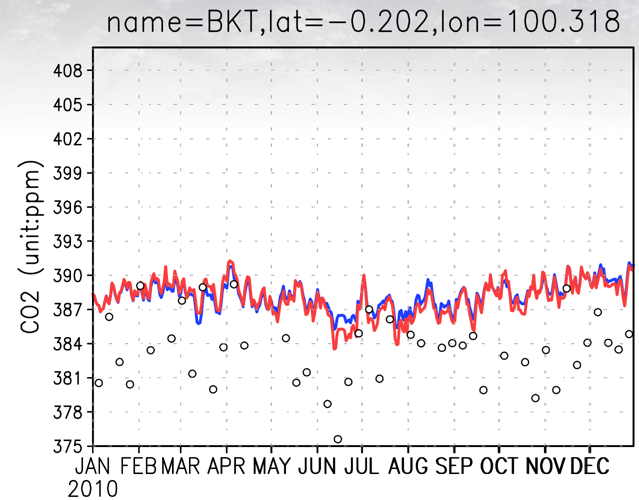

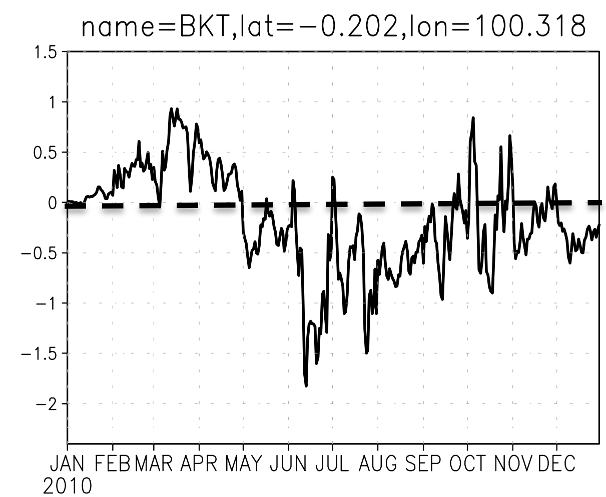

Comparison to surface data

Cape point, South Africa

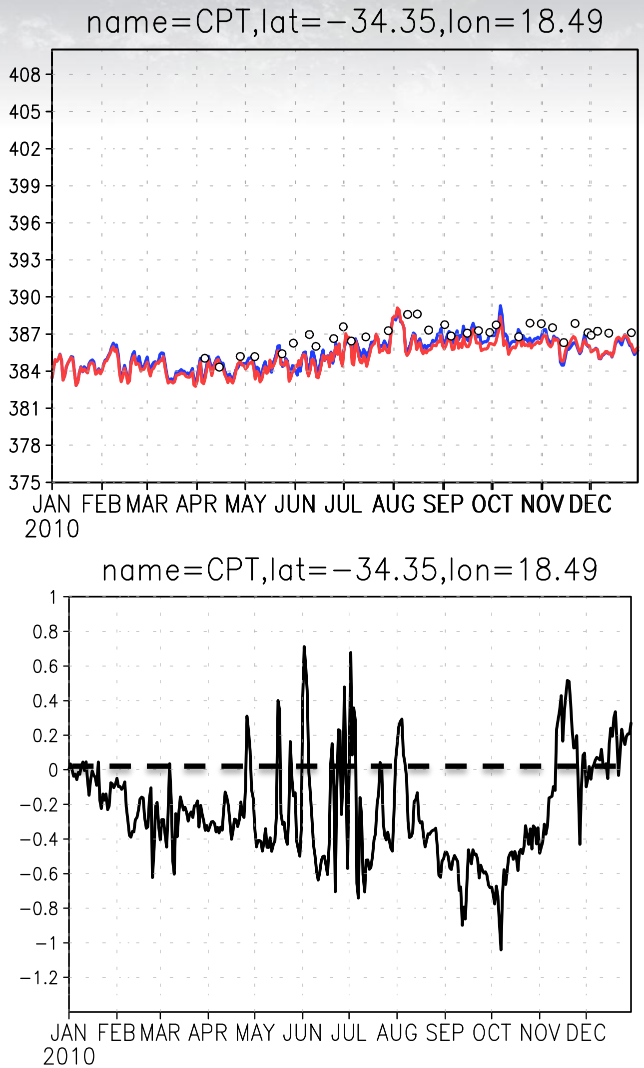

Cold Bay, Alaska, US

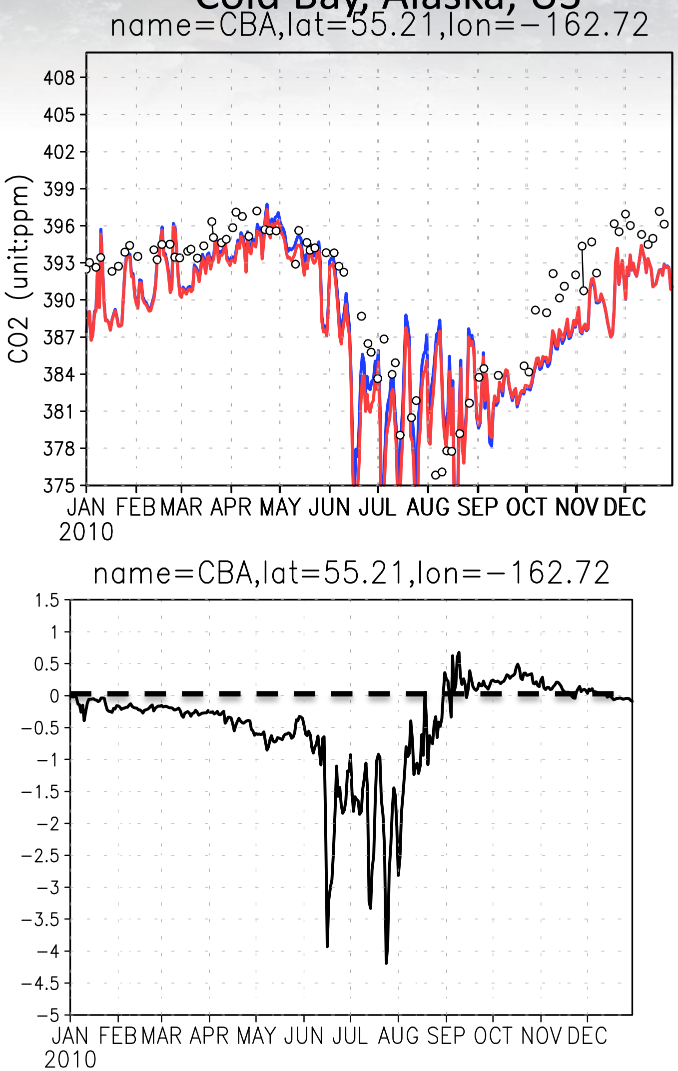

Seasonal prior flux (left panels) and the difference between posterior and prior fluxes

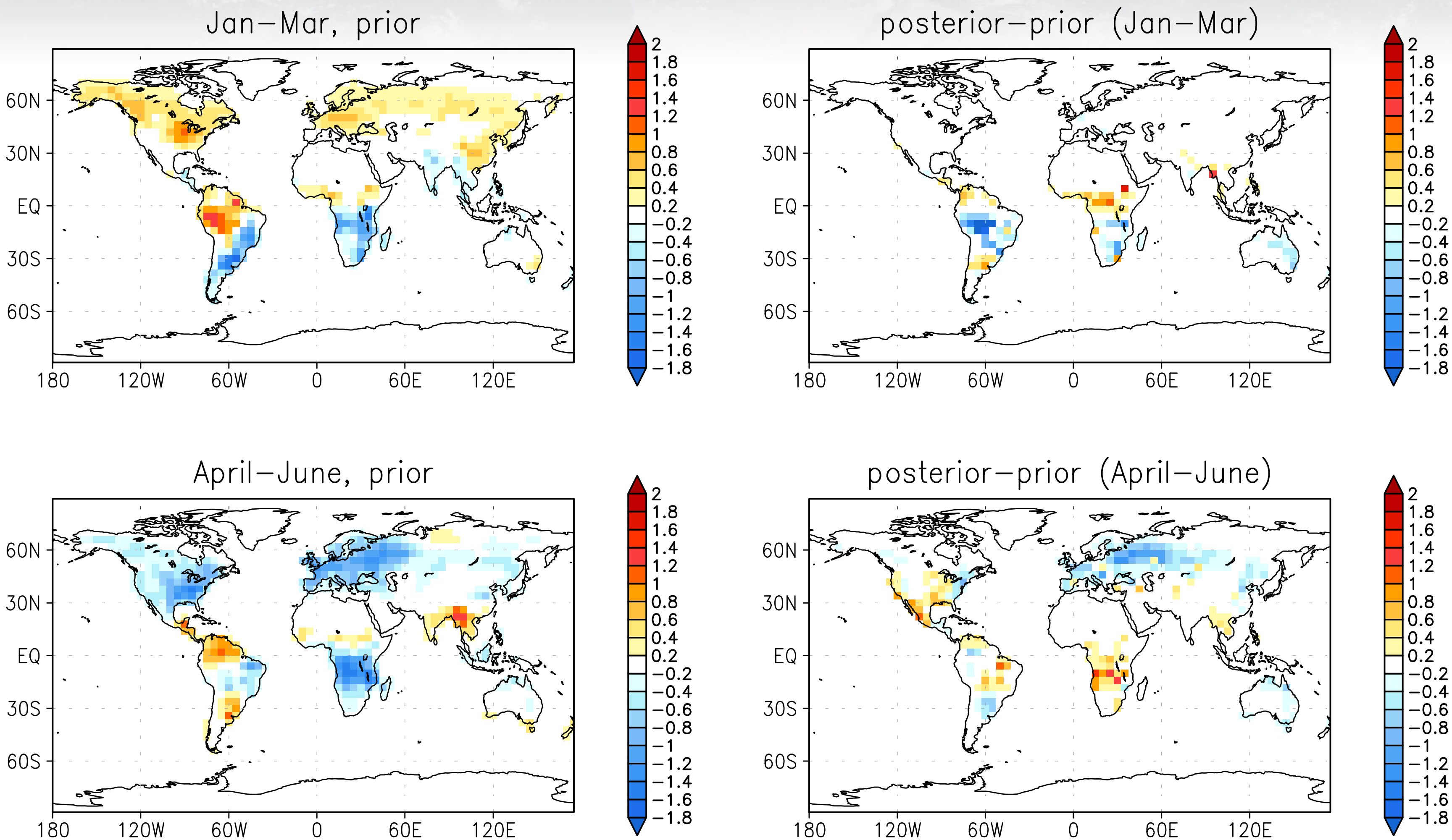

Seasonal prior flux (left panels) and the difference between posterior and prior fluxes

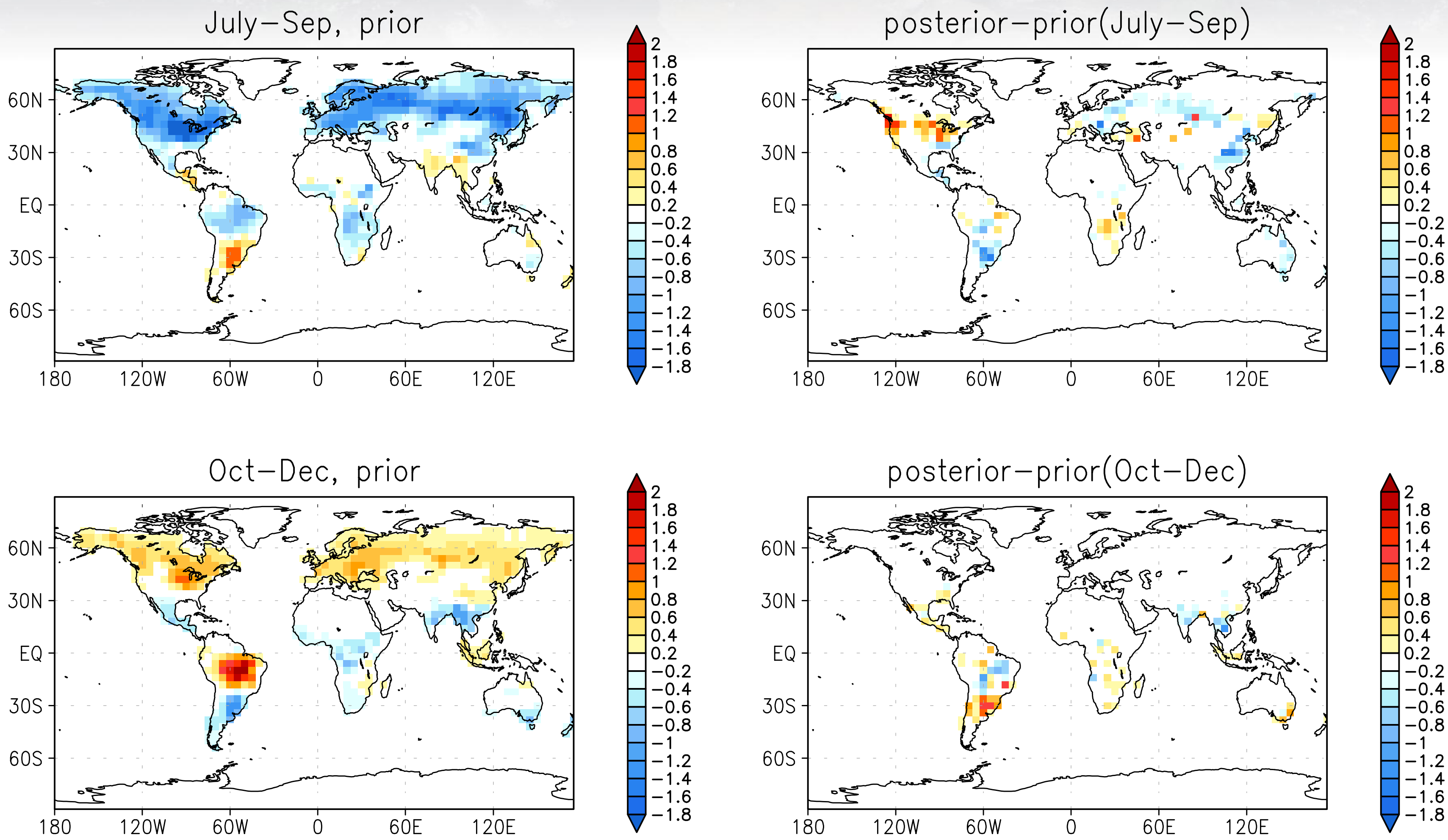

Impact of sampling frequency

(y-h(x))^2 divided by the observation error variance

Chi^2

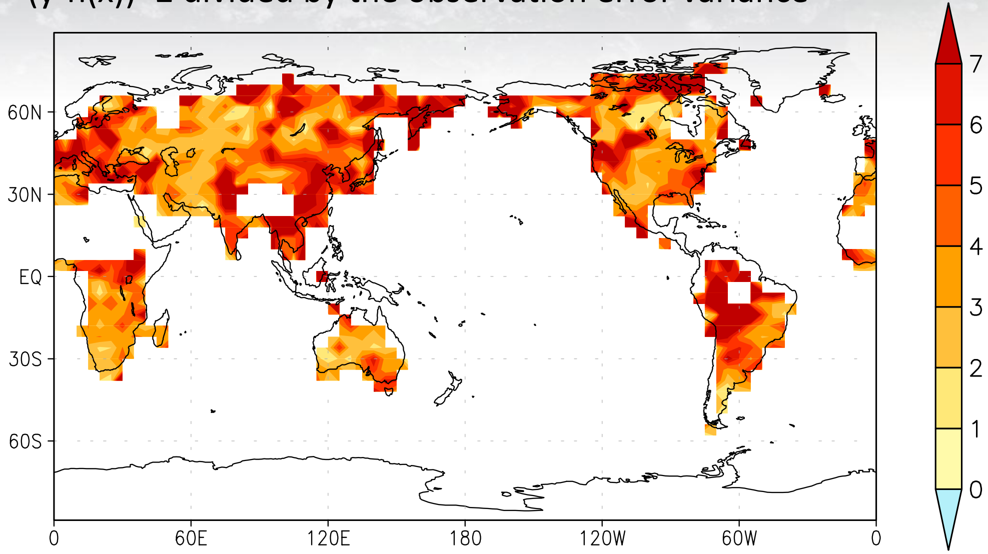

annual total number of observations

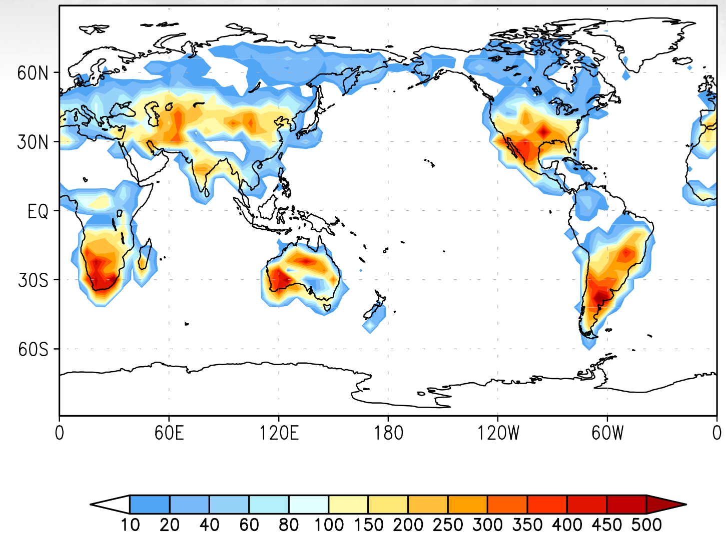

- The locations with high chi-square closely follow the sparse observation locations
- High chi-square is a potential consequence of insufficient sampling.
- Using a small number of samples for attribution could be more vulnerable to model and data error.

Patterns of change

Posterior - prior

The strongest changes happen in the boreal summer over North America and Europe; This is due to both the increase of observations and also the strong variability in the summer.

Jan–Mar 2010 (post–prior) flux (unit: gC/m^2/day)

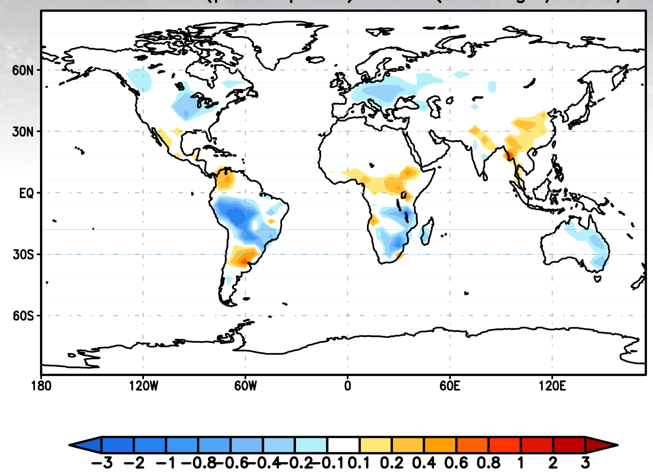

pril–June 2010 (post–prior) flux (unit: gC/m^2/da

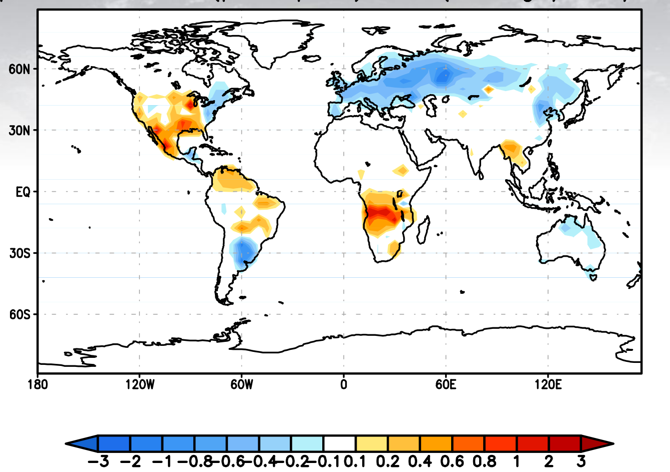

July–Sep 2010 (post–prior) flux (unit: gC/m^2/day)

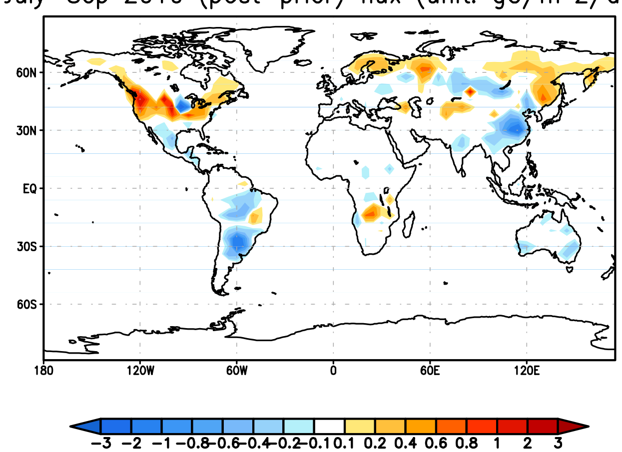

Oct–Dec 2010 (post–prior) flux (unit: gC/m^2/day)